SIMPLIFIED MODEL
FOR REINFORCED CONCRETE BEAMS
UNDER CATENARY ACTION

A Thesis

presented to

the Faculty of the Graduate School

at the University of Missouri-Columbia

In Partial Fulfillment

of the Requirements for the Degree

Master of Science

---

by

RASOLOFOMALALA ANDRY NIRINA

Dr. Sarah Orton, Thesis Supervisor

JULY 2010

The undersigned, appointed by the dean of the Graduate School, have examined the thesis entitled

SIMPLIFIED MODEL

FOR REINFORCED CONCRETE BEAMS

UNDER CATENARY ACTION

presented by Rasolofomalala Andry Nirina,

a candidate for the degree of Master of Science in Civil Engineering,

and hereby certify that, in their opinion, it is worthy of acceptance.

Professor Sarah Orton

Professor Hani Salim

Professor P. Frank Pai

ACKNOWLEDGEMENTS

I would like to thank the Fulbright Visiting Student Junior Staff Development Program for having given me such a great opportunity to complete my degree program in the U.S. and fulfill my life dream of getting my degree in Structural Engineering.

I express my deepest gratitude to my Academic Advisor Assoc. Prof. Sarah Orton for her guidance, advice, criticism, encouragements, and insight throughout the research. I could not have asked for advisors more generous with her time and consideration.

My gratitude is extended to the other faculty members, Prof. P. Frank Pai and Prof. Hani Salim for their valuable suggestions and comments and for serving on my thesis committee.

I also express my thanks and appreciation to my family for their understanding, support and patience during those two years.

Lastly, I am thankful to all professors, staff and friends who have contributed to my education and made my stay at the University of Missouri a memorable and valuable experience.

ABSTRACT

The purpose of this research is to develop simplified models to predict the load displacement behavior for any reinforced concrete beam on the basis of material, geometric, and design parameters. The proposed simplified model includes a beam element and a system of springs that represents the load extension behavior and moment rotation behavior of a reinforced concrete beam element. Spring properties are based on material, geometric, and design parameters. The tensile definition of the axial extension spring is approximated by a steel stress-strain curve modified to account for uneven stress in the steel along the length of the beam. The commercial finite element code ANSYS is used to analyze the models. The results of the models are then compared with experimental tests on reinforced concrete beams, and good agreements are found.

TABLE OF CONTENTS

LIST OF FIGURES

LIST OF TABLES

1. INTRODUCTION

Most Reinforced Concrete buildings are not designed for loading conditions that may lead disproportionate collapse such as gas explosion, blast, foundation failure, vehicle impact, fire, and seismic forces. However, consequences due to disproportionate collapse on structures can be severe when unexpected extreme loading events occur. Collapse of several buildings such as the Ronan Point Apartment Building in England in 1968, the Murrah Building in Oklahoma City in 1995 and the World Trade Center towers in New York in 2001 demonstrated that most casualties are due to building collapse. As a result, research on disproportionate collapse has gained particular attention over the past few years.

ASCE Standard 7-05 defines progressive collapse as the spread of an initial local failure from element to element, eventually resulting in collapse of an entire structure or a disproportionately large part of it (ASCE, 2005). In other words, disproportionate collapse is a chain reaction of failures following damage to a relatively small portion of a structure (Sasani and Kropelnicki, 2007).

Reinforced concrete buildings can resist disproportionate collapse through a variety of mechanisms. These alternate resistance mechanisms include Vierendeel action, catenary action, compressive arch action, membrane action in the floor slab, and contributions from infill walls. Vierendeel action, or frame action, is characterized by rectangular

openings with fixed joints that are capable of transferring and resisting bending moments. Catenary, or membrane action, enables the resistance of gravity forces through tension if the structural member undergoes extreme deflection. Development is highly dependent on continuity of reinforcement. Compressive arch action involves axial restraint of surrounding structure that keeps beams from rotating, forming a compressive arch. Infill walls provide additional stiffness due to nonstructural walls.

This thesis is primarily concerned with catenary action in reinforced concrete beams. Sometimes called cable action, it resists vertical load by mobilizing axial tension throughout reinforced concrete beam. As can be seen in Figure 1-1, catenary action in a reinforced concrete beam is a tensile force that is composed of a vertical and horizontal component due to deflection of the member without any flexural reaction. The vertical component resists the gravity loads while the horizontal component is transferred throughout the building.

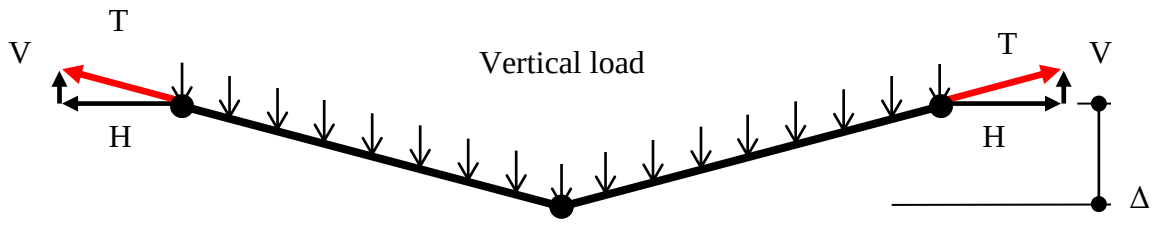

Figure 1-1.Beam under catenary action

T- Tension force

V- Vertical Force resists gravity loads

H- Horizontal force

Δ- Vertical Displacement

Alternate resistance mechanisms in reinforced concrete buildings are not commonly considered in typical disproportionate collapse analysis. Nevertheless, they may provide extra capacity to the building and may prevent a total collapse of the structure in case of extreme loading events. A number of reinforced concrete buildings were able to withstand disproportionate collapse after the loss of one or several supports due to accidental loads because of these actions (Sucuoglu 1994, Sasani et al. 2007). Therefore, investigating alternative resistance mechanisms is significant for life safety in extreme loading events.

1.1 Problem

Presently, there is limited information and research on alternative resistance mechanisms of reinforced concrete buildings. The aim of this research is to contribute to the development and understanding of one of these mechanisms: the catenary action. The problem this thesis seeks to solve is how to define a simplified analysis model to predict the response of a reinforced concrete beam under catenary action.

1.2 Objectives and research approach

The primary objective of the research is to develop simplified models to predict the load displacement behavior for any reinforced concrete beam on the basis of material, geometric, and design parameters. Specifically, this research will develop and implement

in ANSYS simplified models to predict response of reinforced concrete beams under catenary action. The models consider reinforced concrete beams with non-continuous and continuous reinforcement. The simplified models will consist of one beam element with 2-node, three degrees of freedom and one or several spring systems that represent the behavior of the material component of the reinforced concrete beam. The moment rotation response of the beam is modeled through a coupled concrete compression and steel tension springs. The properties of the springs are directly determined from a moment rotation analysis of the reinforced concrete section. Another spring models the axial extension along the beam. The tensile behavior of the axial extension spring is based on a modified stress-strain curve for steel. The curve is modified to take into account the non-uniform distribution of stress along the length of the steel reinforcement. The compression behavior of the axial extension spring will be based on concrete stress-strain curves. Next, the responses from the simplified model are compared and validated using existing experimental data.

1.3 Outline

This research is organized into 5 chapters. Following the introduction, Chapter 2 reviews the relevant literature pertaining to disproportionate collapse in reinforced concrete building, alternative mechanisms resisting disproportionate collapse, models and laboratory testing of reinforced concrete beam under in catenary action. Chapter 3 describes the proposed simplified models development and calibration procedures to predict the response of a reinforced concrete beam under large deformation. Chapter 4

discusses and provides comparison of reinforced concrete beams under large deformation response observed in the laboratory and simulated using the proposed models results while chapter 5 present the conclusions of this research. The document concludes with a list of the references cited in this research.

2. LITERATURE REVIEW

Previous investigations have been carried out to better understand catenary action. They include laboratory testing and analysis to predict and quantify the behavior of reinforced concrete and steel members under large deformation. This chapter will review relevant literature pertaining to disproportionate collapse in reinforced concrete building, alternative mechanism resisting disproportionate collapse, models and laboratory testing of reinforced concrete beam under in catenary action.

2.1 Disproportionate collapse in buildings

A number of structures have experienced disproportionate collapse while others did not after the loss of one or several supports due to extreme loading events. The following section gives some notable examples of disproportionate and non-disproportionate failures of reinforced concrete buildings which happened in the past.

2.1.1 Examples of disproportionate collapse

The collapse of the Ronan Point Tower in 1968 in Canning Town, London is one of the most famous cases of disproportionate collapse. The incident was initiated by a gas-stove leak on the 18th floor in apartment 90. The ultimate result was a collapse of the corner bay of the building from top to bottom, Figure 2-1. Ronan Point was a 22-story residential apartment tower consisted of precast panels joined together without a structural frame. Due to poor connections between the walls and floor, no alternate load paths to redistribute forces existed in the event of a partial collapse. Since the collapse of

the southeast corner of Ronan Point, changes to building codes to prevent the recurrence of such tragedies have been initiated in the United Kingdom and throughout the world (Pearson and Delatte, 2005). For example, in the United Kingdom precast concrete structures are required to be tied together so that they can either provide an alternate load path or a specific local resistance to withstand an abnormal load (NIST, 2007; Breen, 1975).

Figure 2-1.Ronan Point building after collapse (Nair, 2004)

Another example of disproportionate collapse is the Alfred P. Murrah Building in Oklahoma City, Oklahoma. The Murrah building was destroyed by a bomb on April 19, 1995 (FEMA 1996). The bomb, in a truck at the base of the building, destroyed or badly damaged three columns. Loss of support from these columns led to failure of a transfer

girder. Failure of the transfer girder caused the collapse of columns supported by the girder and floor areas supported by those columns. The result was a general collapse; about half of every floor was lost over the full height of the building, Figure 2-2 (Nair, 2004).The building was designed with non-continuous reinforcement in both the positive and negative moment reinforcement in the beams. If the building had been detailed as a special moment frame the collapsed area of the structure could have been reduced 50% to 80% (Corley, 2004). The extent of the collapse prompted studies of progressive/disproportionate collapse and development of new design guidelines for important buildings (Nair, 2004).

Figure 2-2.Murrah Federal Office Building after 19 April 1995 attack (Crawford, 2002)

2.1.2 Examples of non-collapse buildings

While Ronan Point and the Murrah Federal Office Building are some of the most famous examples of reinforced concrete building which have experienced disproportionate collapse due to extreme loading events, many other structures have suffered severe damage but did not lead to disproportionate collapse.

One example is the partial collapse of the Pentagon Building in Washington, D.C. on September 11th 2001. A plane was flown into the first floor of the building and destroyed 30, first-floor columns and damaged about 20 others along a path that extended approximately 75 ft wide by 230 ft long through the first floor, Figure 2-3 (Mlakar et al., 2003). Even with the extensive damage to many columns in the first floor, the upper stories remained intact for more than 20 minutes until they collapsed due to fire after the airplane impact. According to the Pentagon Building Performance Report (Mlakar et al., 2003), reasons for the performance of the building are:

- "Redundant and alternative load paths of the beam and girder framing system;
- Short spans between columns;
- Substantial continuity of beam and girder bottom reinforcement through the supports;
- Design for 150 psf warehouse live load in excess of service load;
- Significant residual load capacity of damaged spirally reinforced columns;"

Figure 2-3.Pentagon building after the crash damage (Mlakar et al., 2003)

Another example is a typical reinforced concrete six-story office building (Figure 2-4) damaged by a steam boiler explosion reported by Sucuoglu et al. (1994). Sucuoglu et al. investigated the redistribution paths of released forces resulting from a column failure and identified the basic structural defense mechanisms developed in the damaged building frame. One of the findings of the study showed that non-load-bearing infill wall panels provides reserve strength and prevents the progressive failure of the structure.

Figure 2-4. Front View of Reinforced Concrete Building Damaged by System Boiler Explosion (Sucuoglu et al., 1994).

One last example is the limited vertical drift (deformation) of the Hotel San Diego in San Diego, Figure 2-5 and Figure 2-6. Scheduled for demolition, Hotel San Diego was a six-story reinforced concrete frame structure built in 1914. It had a non-ductile reinforced concrete frame structure with hollow clay tile exterior infill walls. In order to determine the collapse resistance of the building, Sasani and Sagiroglu (2007) carried out an experimental evaluation following predefined initial damage of the structure. The initial damage was caused by the simultaneous explosion (removal) of two adjacent exterior columns, one of which was a corner column. Based on experimental data, the development of bidirectional Vierendeel (frame) action was identified as a major

mechanism in redistribution of loads. This mechanism with increased stiffness from infill walls contributed to resisting the failure of the building.

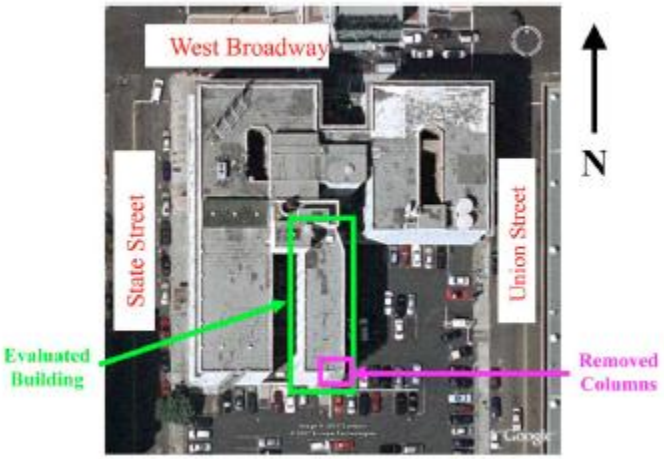

Figure 2-5. Aerial view of Hotel San Diego

Figure 2-6. South-east view of Hotel San Diego

2.2 Modeling of reinforced concrete beams under catenary action

Previous research provides a number of models for use in simulating the response of reinforced concrete elements under catenary action. In general, these previously proposed models range from relatively simple to complicated equations based on the fundamental concepts of equilibrium, compatibility, and material characteristics.

Regan (1975) developed a simple equation to predict the catenary behavior following the loss of support of a reinforced concrete element based on the load extension characteristics of the members and simple equilibrium. For static equilibrium the equation is:

$$Ha = \frac{qL^2}{2} \qquad (2\text{-}1)$$

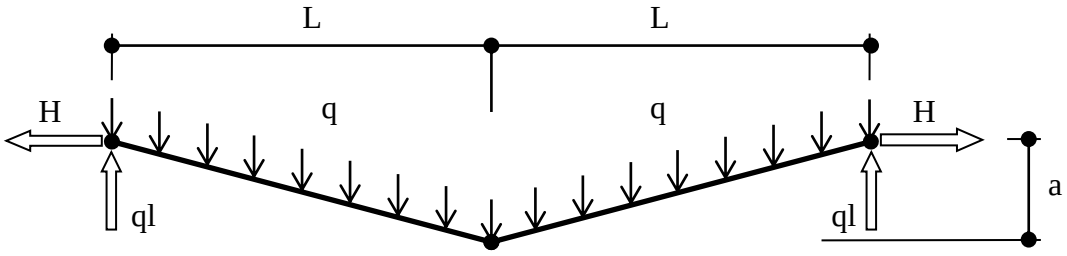

Figure 2-7. Free body diagram of Regan's Model (Regan, 1975)

Where H is the axial tension in the catenary, q is the distributed load on the beam, L is the beam length and a is the central deflection of the bam.

The axial extension of the beam (ΔL) required by geometry is:

$$\frac{\Delta L}{L} = \frac{1}{2}\left(\frac{a}{L}\right)^2 \quad (2\text{-}2)$$

For the bi-linear deflected form of Figure 2-7.

The final component to the analysis is to define the axial extension of the beam which will define the relationship between H and $\frac{\Delta L}{L}$. This relationship depends on the reinforcement details. Regan defined the slip (N_{slip}) of the reinforcement at the joint as varying between 0 to the ultimate extension of joint $(\Delta L)_u$.

$$N = N_{slip} \text{ for } 0<\Delta L<\Delta L_u \quad (2\text{-}3)$$

This gives a predicted load, axial force, deflection relationship of:

$$a = \frac{ql^2}{2N_{slip}} \qquad \text{for } 0<a<L\sqrt{2\frac{\Delta Lu}{L}} \quad (2\text{-}4)$$

Regan found reasonably good agreement with the shapes of the load – deflection curves obtained in catenary tests but it was difficult to predict ultimate load because of difficulty in predicting the ultimate extension of the joint $(\Delta L)_u$.

Orton (2007) developed a similar set of equations that were based on equilibrium, geometry (compatibility), and the axial extension of concrete beams. For a beam without continuous reinforcement, a hinge will open at the column line which has no moment capacity. Therefore, the equilibrium of the beam, with two point loads (see diagram in Figure 2-8), will be:

$$M + A\Delta - P\frac{L}{2} - P\frac{L}{2} = 0 \quad (2\text{-}5)$$

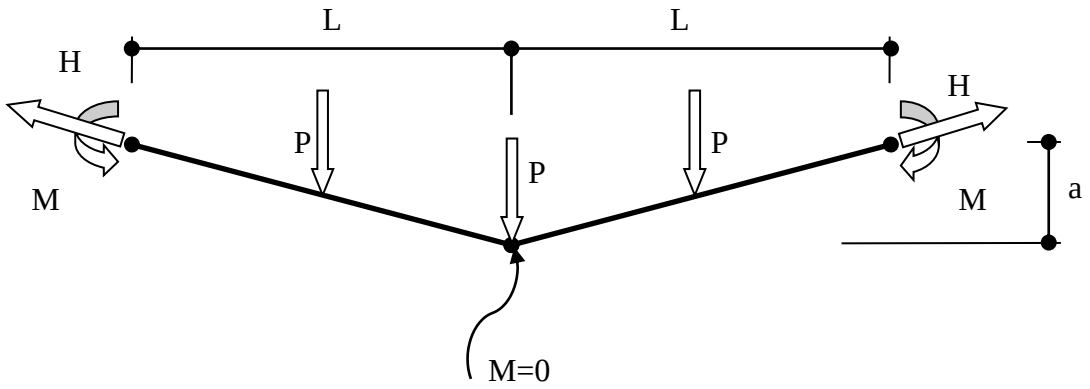

Figure 2-8. Free body diagram of Orton's Model (Orton, 2007)

By rearranging that equation, the value of axial force becomes:

$$H = \frac{PL-M}{a} \tag{2-6}$$

Where M is the nominal flexural capacity of the hinge at the support, A is the axial tension, Δ is the center deflection, P is the point load, and L is the length of the modeled half of the beam.

For the compatibility geometry, the extended length of the beam (L+ΔL) is related to the deflection Δ and original length L by the Pythagorean Theorem. Therefore, the equation becomes:

$$\Delta = \sqrt{(L + \Delta L)^2 - L^2} \tag{2-7}$$

For axial extension, Orton considered three components: due to rotation of beam δ_g, support movement δ_s, and elongation in the beam δ_e. The equation has the following form:

$$\Delta L = \delta_g + \delta_s + \delta_e \tag{2-8}$$

The axial extension of the beam was divided into contributions for different sections of the beam based on the approximation of yielding of the reinforcement elongation along the length of the beam. Using these equations, Orton was able to replicate the vertical load versus deflection and the axial load versus deflection responses of the experimental study.

Izzudin (2004) proposed an analytical model for lightly reinforced members under fire conditions subjected to axial restraint. The model accounts for the compressive arch and tensile catenary stages, bond-slip, yielding, rupture of steel reinforcement and effect of elevated temperature. He concluded that there is a compressive arch action up until a deflection equal to the depth of the beam. In addition to that, he found out that the scale of the catenary effect is dependent on the beam depth and the support axial stiffness. Model to predict deflections and catenary forces in steel beams at elevated temperatures also was proposed by Yin and Wang (2003).

2.3 Experimental tests of reinforced concrete beams under catenary action

Along with the modeling of reinforced concrete under catenary action, relatively few experimental investigations have been carried out to study the response of reinforced concrete elements subjected to large deformation. One of earliest works was conducted by Regan (1975) at Imperial College in London. He tested precast floor strips 14 in. to 28 in. wide and 18 ft long with a central joint between two 9 ft planks representing a lost support. The specimens comprised a 2 in. thick precast panel and a 2 in. thick cast-in-

place topping. Details of the ties between the panels varied according to the specimens' width, Figure 2-9.

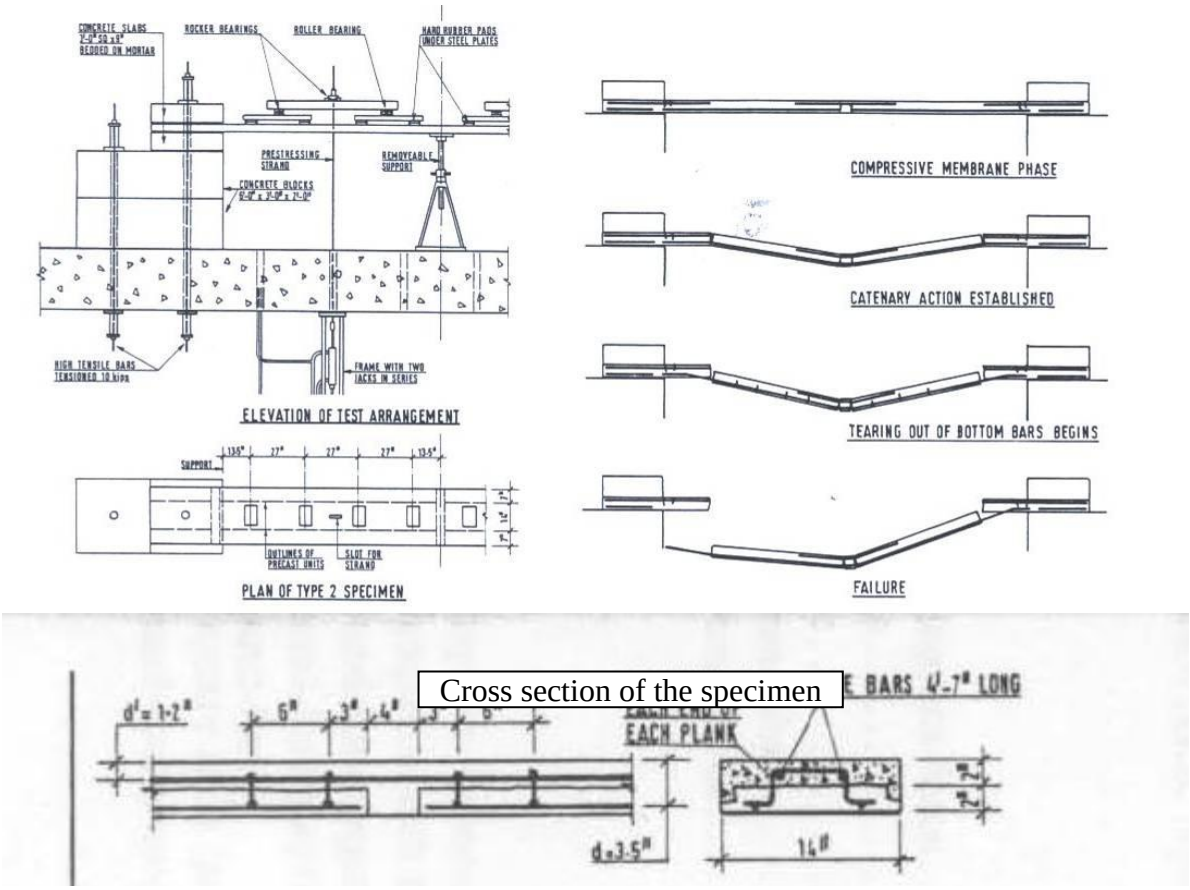

Figure 2-9. Arrangement for PCL catenary test (Regan, 1975).

In all the tests, it was observed an initial compressive arch phase followed by catenary action phase. The majority of the beams failed by tearing out of the bottom bars near the supports at a deflection of 5 to 7% of the double span length (test #5 in Figure 2-10). However in a few cases, the end cantilevers yielded before any tearing of the bottom bars began. In these cases ultimate central deflections were about 10% of the doubled span

and collapse was caused by fracturing of the end ties, due to limited rotation between the specimen and its supports (test #3 in Figure 2-10).

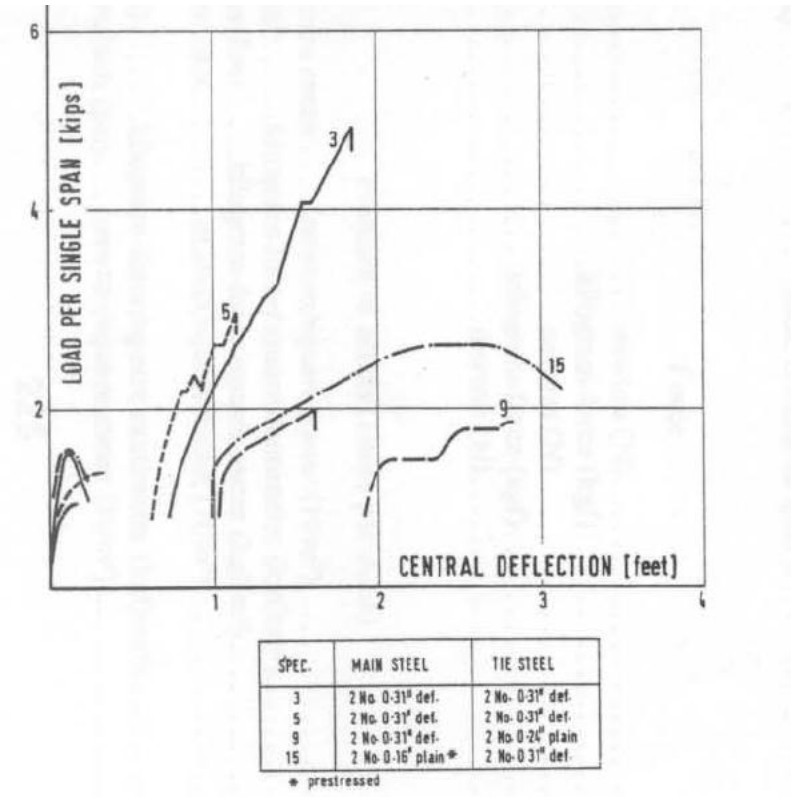

Figure 2-10.Results of catenary tests of precast floor strips (Regan, 1975)

Based on the tests results, Regan concluded that "successful development of a catenary action requires that the members in question posses not only tensile strength but also ductility, which is largely determined by the detailing of the longitudinal reinforcement."

Sasani and Kropelnicki (2007) carried out another experimental program to evaluate the behavior of a 3/8 scaled model of a continuous perimeter beam in a reinforced concrete

frame structure following the removal of a supporting column. They also used a detailed finite element model to capture the behavior of that beam subjected to large deformation using ANSYS. The beam was 13 ft 8¼ in. long by 12 in. by 20 in. It was constructed with fixed boundary conditions. Reinforcement of grade 75 ksi was used along with concrete compressive strength of 6 ksi. Figure 2-11 shows the reinforcement detailing of the beam. The test was conducted utilizing displacement control at the center span (Sasani and Kropelnicki, 2007).

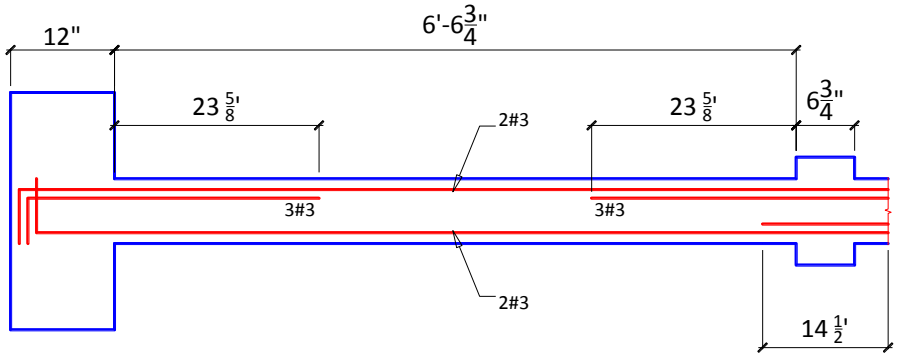

Figure 2-11. Reinforcement detailing of the experimental beam (Sasani and Kropelnicki, 2007).

As shown in Figure 2-12 and from the tests results, it was found that the two bottom bars fractured at vertical displacements of about 6.0 in. and 7.5 in. Furthermore, by satisfying the integrity requirements of ACI-318, they found that catenary action developed in the top reinforcement following the bar fractures. Finally, the beam end rotation at the conclusion of the test was measured at about 11 degrees (slope of about 20%) (Sasani and Kropelnicki, 2007).

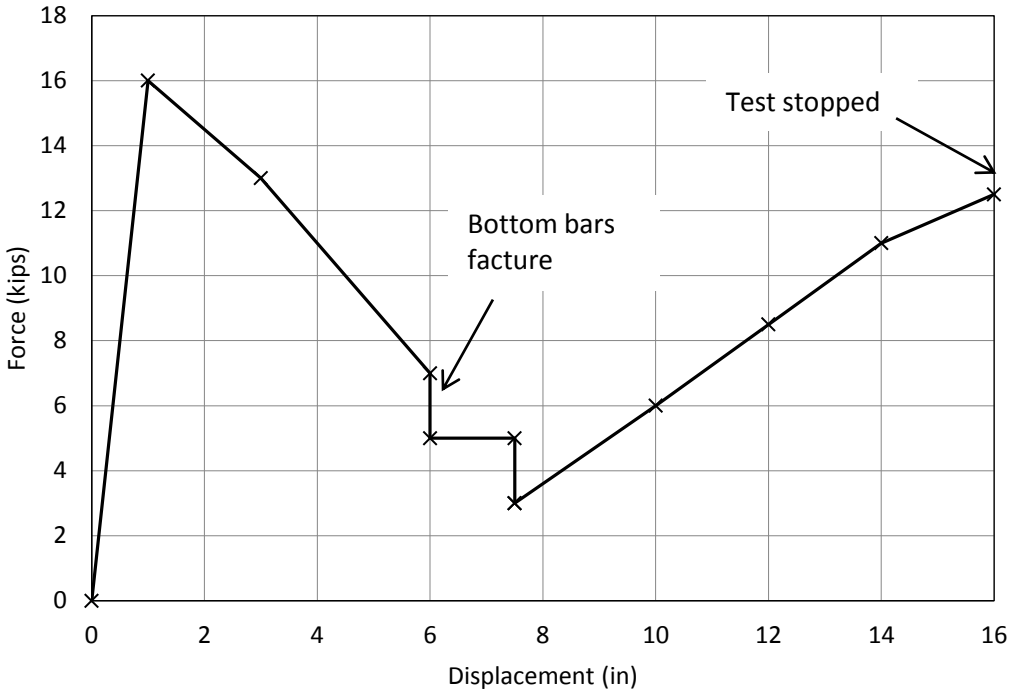

Figure 2-12. Force – Displacement relationship (Sasani and Kropelnicki, 2007).

In 2007, Orton tested eight beams evaluate different load paths to develop continuity and catenary action in reinforced concrete beams. The experiments consisted of test on half-scale reinforced concrete beams that measured 30 ft long with a cross-section of 6 in. by 12 in. The reinforcement consisted of #3 (0.11 in2) and #4 (0.2 in2) reinforcing bars equivalent to half-scale versions of the prototype beam. Figure 2-13 shows the reinforcement detailing of the beam. (Orton, 2007).

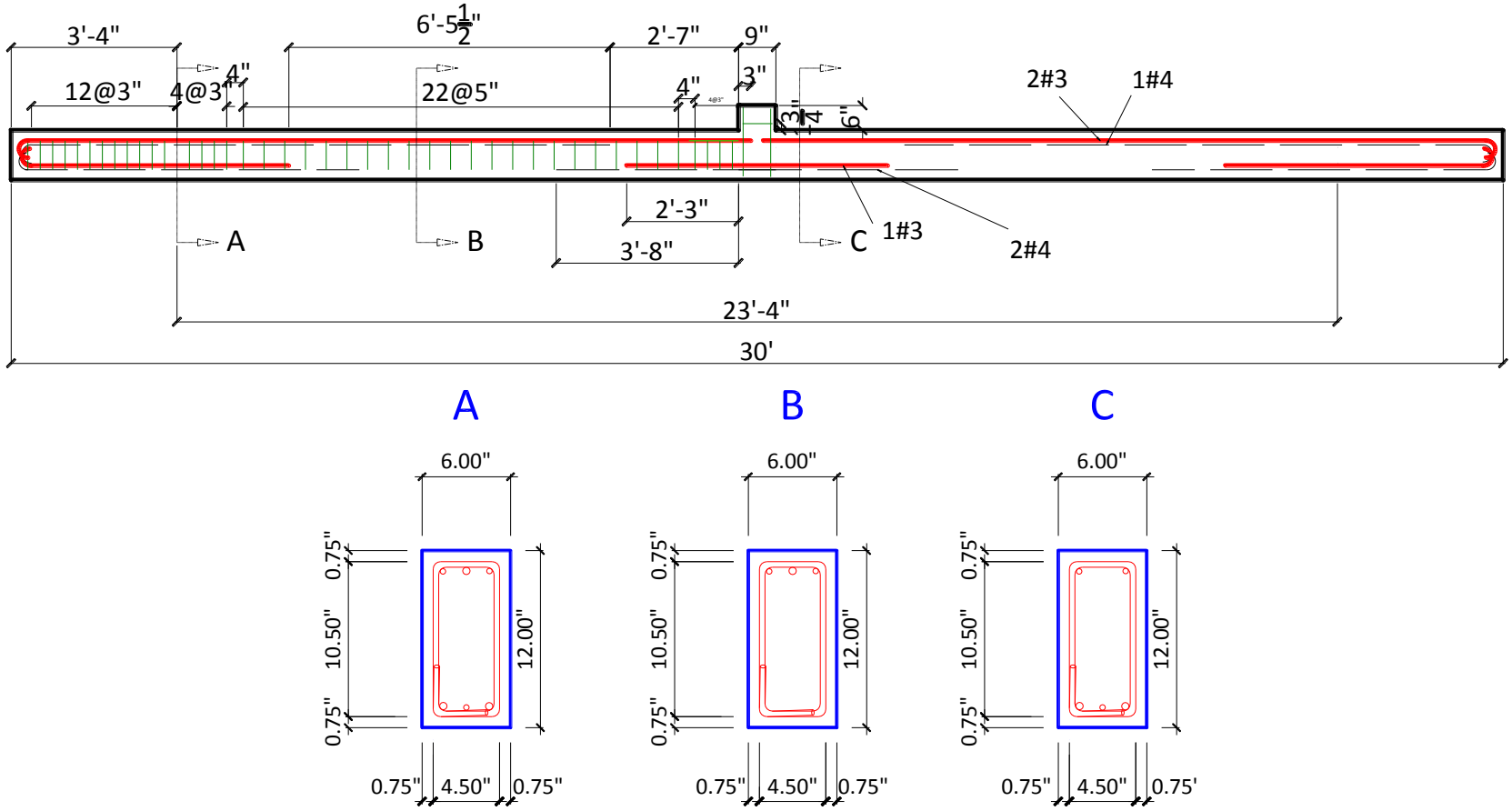

Figure 2-13. Reinforcement design of test specimen (Orton, 2007)

One test (NR-2) found that beams without continuous reinforcement were able to transfer tension forces for catenary action from the positive moment steel to the negative moment steel through stirrups Figure 2-14

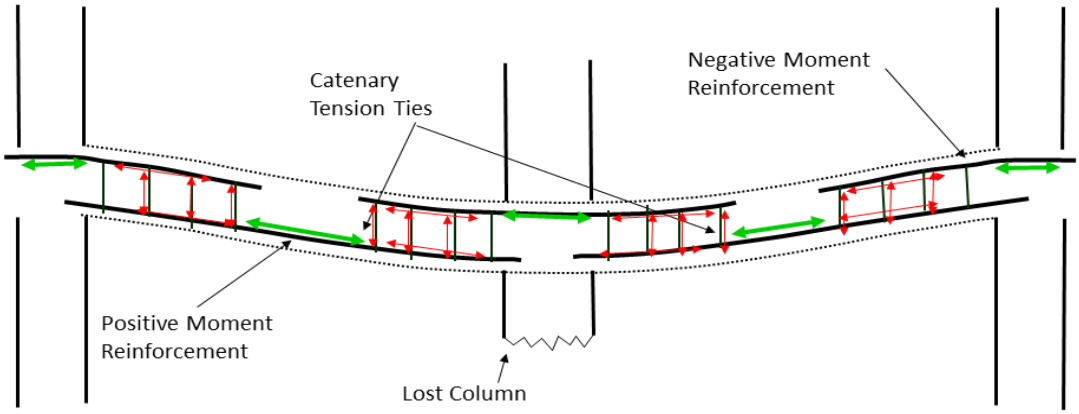

Figure 2-14. Transfer of catenary forces through stirrups (Orton, 2007)

The axial load and vertical load versus deflection response (Figure 2-16) shows a compressive arch phase until about 16 in. of deflection, and then a catenary tension phase. During the catenary tension phase the test specimen was able to carry 2.5 times the load that is was able to carry in flexural action. The test was then stopped at 25 in. of deflection due to limitations in the test setup (Figure 2-16).

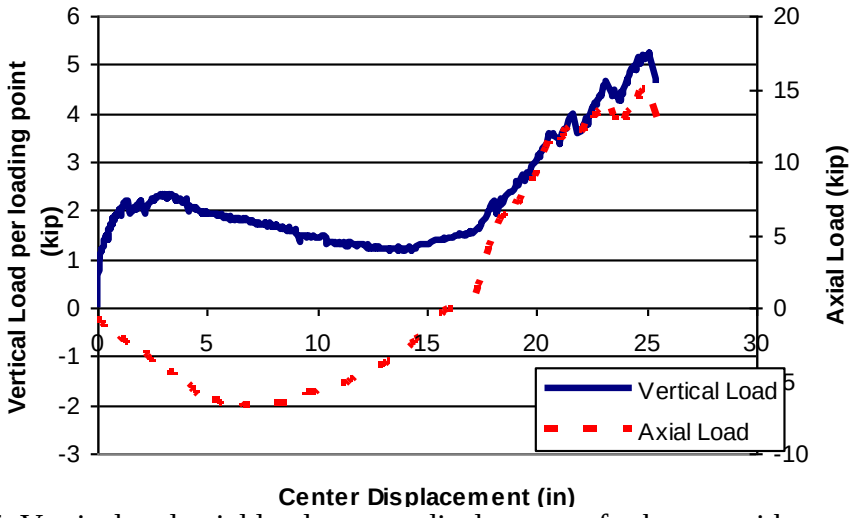

Figure 2-15. Vertical and axial loads versus displacement for beams without continuous reinforcement (Orton, 2007).

Figure 2-16. Photo of test NR-2 under catenary action

Another test (CR-1) found that a beam with continuous steel reinforcement (equal to that required by current version of the ACI code) was not able to carry a load corresponding to disproportionate collapse resistance before continuous reinforcement fractured due to

limited ductility in the beam in the positive hinge region. After failure of the positive moment, the negative moment steel fractured as well.

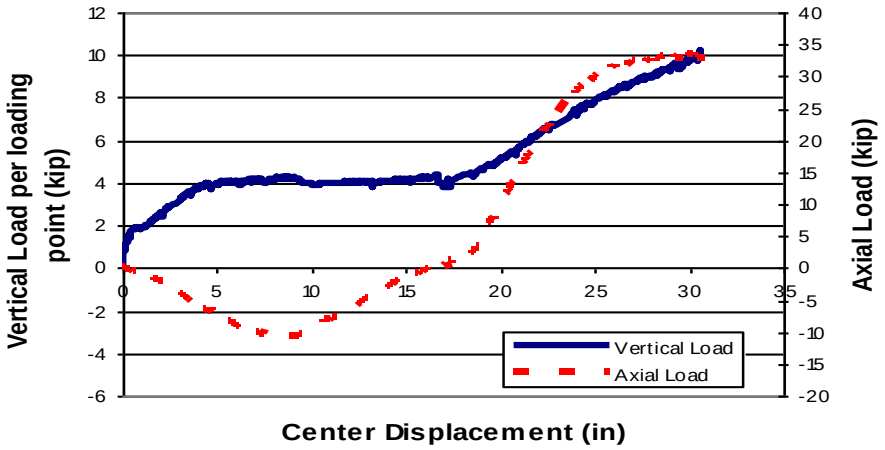

Figure 2-17. Vertical and axial loads versus displacement for beams with continuity provided by CFRP sheets (Orton, 2007).

Figure 2-18. Photo of test PM-2 under catenary action

Orton conducted two more tests where continuity of the negative moment reinforcement was provided by external CFRP sheets. For these beams the positive moment reinforcement was discontinuous at the center column line. This allowed the hinge at the center column to open freely, and all catenary tensile forces to be carried by the negative

moment steel and the CFRP, Figure 2-18. For these beams the moment rotation capacity near the support provide some vertical load carrying capacity. As the beam continued to rotate, the load remained nearly constant then increased once the beam went into catenary action at about 17 in. of displacement.

Orton concluded that catenary action begins after the beam has formed a failure mechanism, or the beam is no longer able to sustain additional vertical loads in a flexural manner. Orton further mentioned that a reinforced concrete beam can be modeled a rigid rectangular blocks between the hinge locations and the deflection at which catenary action begins is directly dependent on the height of the beam. Finally, Orton found that the stiffness, or slope of the load-deflection curve, is dependent on the axial elongation of the beam, which is largely dependent on the length of the beam (determines elongation due to geometry) and yielding in the beam (determines beam elongation).

More recently, Yi and Kunnanth (2008) conducted a static experimental study to investigate progressive failure of a reinforced concrete frame due to the loss of a lower story column. They tested one-third scale model of a four-bay and three-story representing a segment of a larger planar frame structure with continuous positive reinforcement, Figure 2-19.

Figure 2-19. The tested four-bay and three-story one-third scale model representing a segment of a larger planar frame structure (Kunnanth, 2008).

The experiments and the analyses results indicated that three phases were experienced during the disproportionate collapse process: elastic, plastic, and catenary phases, Figure 2-20.

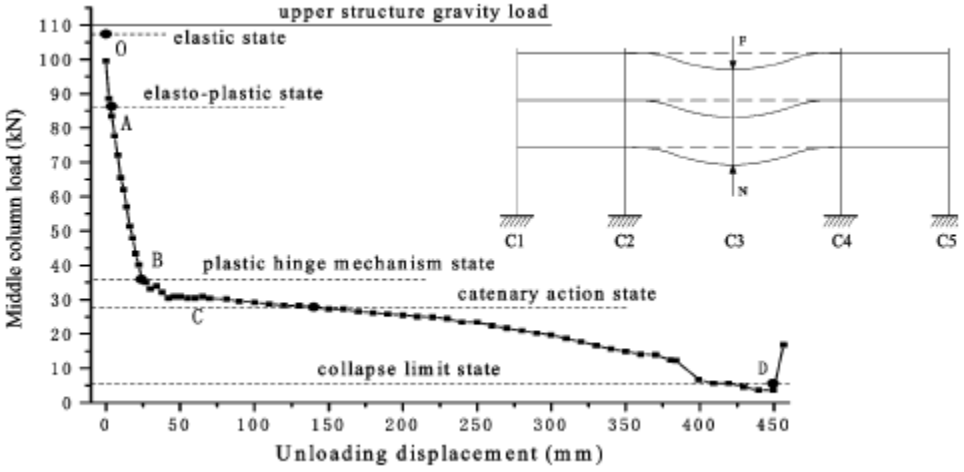

Figure 2-20. Middle column load versus unloading displacement of failed middle column. (Yi and Kunnanth, 2008)

Based on observations and findings from the experimental study, the following conclusions were drawn:

- The catenary action depends on uniform extension of the reinforcing bars.
- The calculated capacity of the frame based on the plastic limit state was approximately 70% of the tested failure capacity if catenary effects are also included.
- The beam catenary mechanism can be considered as an alternative load path and can resist additional loads.

3. MODELLING OF REINFORCED CONCRETE BEAM UNDER CATENARY ACTION

This chapter gives a brief background on catenary action and explains the procedure followed to develop the simplified model. The implementation of the models in ANSYS will also be covered.

3.1 Response of a reinforced concrete beam under catenary action

Catenary action is a tensile force that resists vertical loads by mobilizing axial tension throughout the beam. This action may be capable of adding to the collapse of the resistance of reinforced concrete buildings. In reinforced concrete beams, previous research has shown that catenary action depends on beam geometry, material properties, reinforcement detailing, axial restraint provided by surrounding structure, and axial extension in the beam.

Orton (2007) found that catenary action will not begin until the beam has reached a deflection equal to the height of the beam. This is due to the fact that the concrete beam behaves as a rigid block. As the beam rotates, the corners of block push outward until it reaches the length of the diagonal of the beam (Figure 3-1).

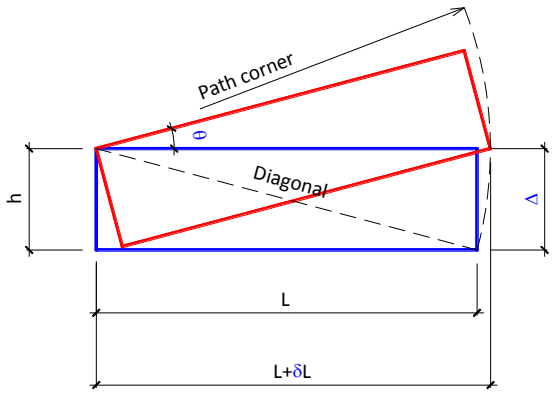

Figure 3-1. Rotation of rigid block (Orton, 2007)

Catenary action also depends on reinforcement detailing and properties. Beams without continuous reinforcement can develop catenary action by transferring forces through the stirrups (Figure 3-2). However, this causes greater of axial elongation in the beam due to shear deformations as the tensile force is transferred from one layer to another. Beams with continuous can transfer directly the axial extension through the line of reinforcement if the reinforcement does not fracture due to limited rotational ductility before the onset of catenary action (Figure 3-3).

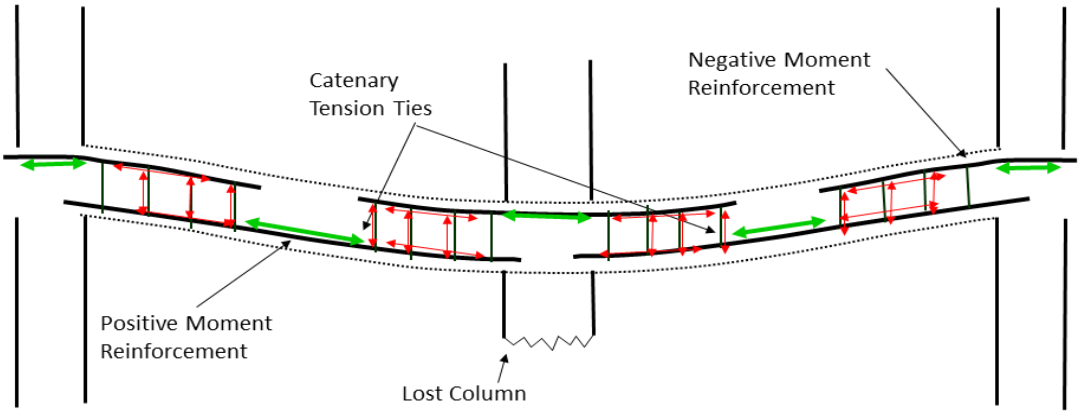

Figure 3-2 . Transfer of catenary action forces through stirrups (Orton, 2007)

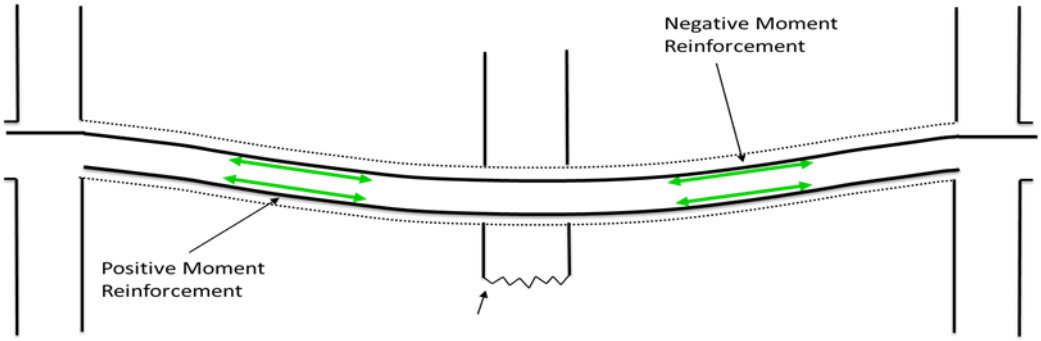

Figure 3-3. Catenary forces provided through the positive and negative moment reinforcement (Orton, 2007)

Also important are reinforcement details in the plastic hinge region. Regan (1975) and Orton (2007) stated that "successful development of catenary action requires that the members in question possess not only tensile strength but also ductility, which is largely determined by the detailing of the longitudinal reinforcement." The ductility they mentioned pertains to, in part the ability of the concentrated rotation locations (hinges) to not fracture the rebar before catenary action is developed.

Catenary action also depends on development of axial restraint. Orton (2007) mentioned that any axial movement that does not require axial force such as extension due to geometry or slip in the connection must be overcome before catenary action can develop. Therefore, catenary action will be limited until the beam is sufficiently restrained axially.

The amount of axial tension and beam deflection is highly dependent on the axial extension of the beam (Orton, 2007). The extension is comprised of primarily of elongations in the reinforcement, but also depends on shear deformations in the concrete

if the reinforcement is not continuous. Furthermore, due to the non-uniform design of the reinforcement along the length of the beam and loading conditions imposed by catenary action, the axial stress in the reinforcement varies along the beam. This variation makes it difficult to determine the axial extension of a reinforced concrete beam under catenary action and will be closely evaluated in this research.

3.2 Proposed simplified model

To simulate a reinforced concrete beam behavior under catenary action, a simplified model is developed based on available test data, material, and geometric parameters. The proposed simplified model uses two-dimensional nonlinear elements. One model considers continuous reinforcement and the other model considers non-continuous reinforcement. The models are composed of one beam element with 2-node, three degrees of freedom at each node and one or several spring systems that represent the behavior of the material component of the reinforced concrete beam. Figure 3-4 and Figure 3-5 show the basic components of the proposed model for reinforced concrete beam with non-continuous and continuous reinforcement. The models differ slightly according to the geometry, the reinforcement detailing and the axial restraint. The beams in Figure 3-4 and Figure 3-5 were tested in an inverted position.

The first model considers a specimen without continuous reinforcement. For this specimen, hinges will develop at where the reinforcement terminates. This occurs at the end of the negative moment reinforcement on the left side of the beam, and the end of the

positive moment reinforcement where it extends only 6” into the column (positive moment reinforcement will pull out of column due to insufficient development length). These hinges have no moment resistance. Therefore, the model is simply comprised of springs that represent the support movement and axial elongation of the beam. The effects of geometry in the model are represented by a rigid beam element that represents the diagonal of the concrete block.

For beams with negative continuous moment reinforcement, hinges with moment resistance can develop and must be accounted for in the model. In Figure 3-5 this occurs at the left hand side of the beam. On the right side the positive moment reinforcement will pull out of the column. For most beams, even if the positive moment reinforcement was continuous, due to limited rotational ductility at that section, the positive moment reinforcement would fracture prior to the onset of catenary action. This was the case in the specimen tested by Sasani and Kropelnicki (2007).

a)

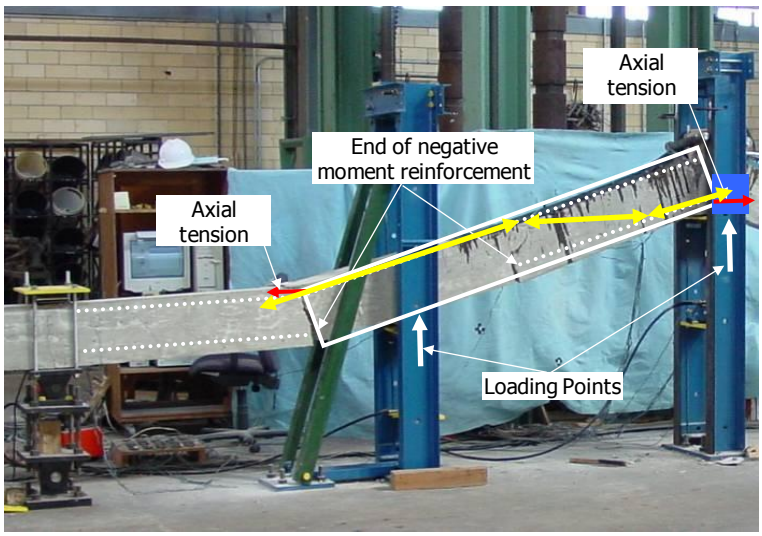

b)

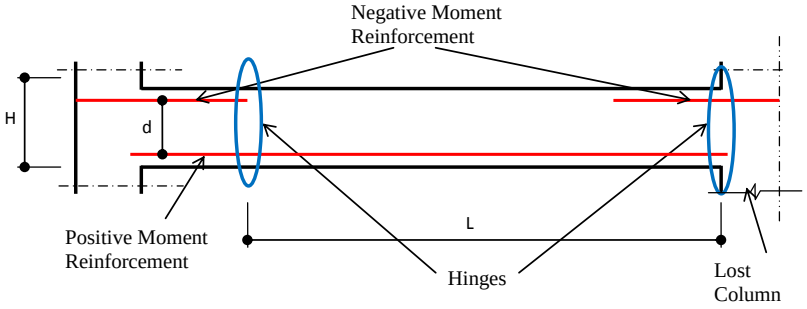

c)

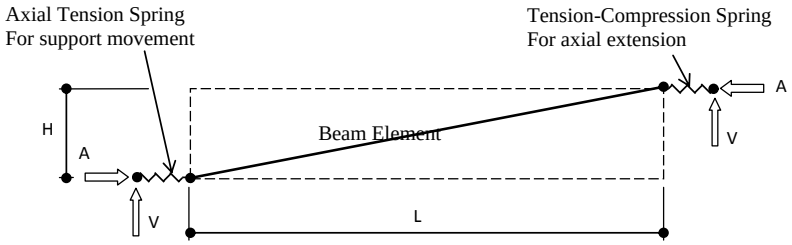

Figure 3-4. a. Reinforced concrete beam with non-continuous reinforcement Orton 2007).
b. Schematic of Reinforced concrete beam with non-continuous reinforcement.
c. Modeling of a reinforced concrete beam with non-continuous reinforcement.

a)

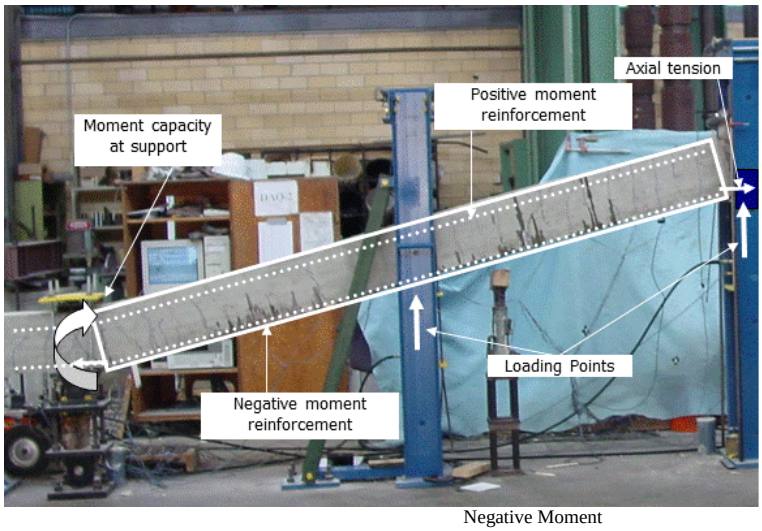

b)

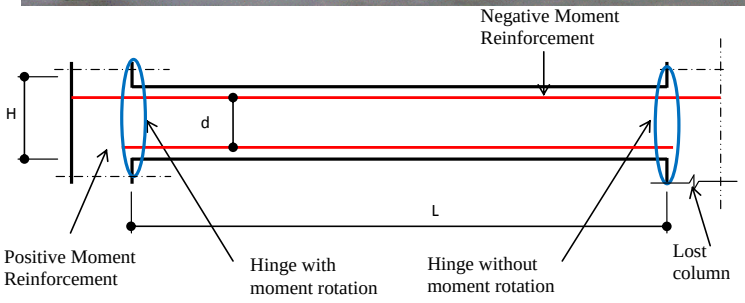

c)

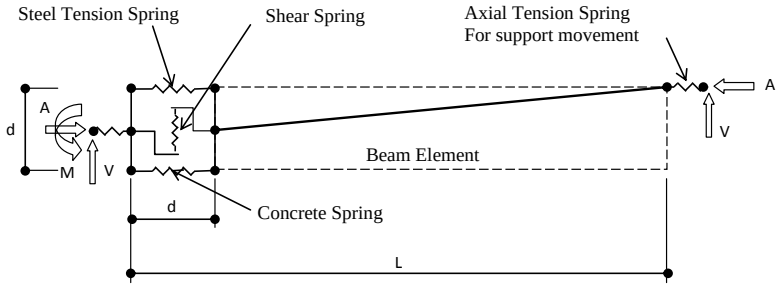

Figure 3-5. a. Reinforced concrete beam with continuous reinforcement (Orton 2007).
b. . Schematic of Reinforced concrete beam with continuous reinforcement.
c. Modeling of a reinforced concrete beam with continuous reinforcement.

3.3 Definition of the elements of the simplified model

Constitutive relationships are developed to define the load deformation response of the model on the basis of available test data, material, geometric, and design parameters. The results of the experimental investigation by Orton (2007), and Sasani and Kropelnicki

(2007) are used as a basis for validating the different elements of the models. They provide the most complete and comprehensive data set for developing the models. Assumptions based on engineering judgment were also used.

3.3.1 Beam Element

The beam element represents the effect of the geometry in the model. It is represented by a diagonal of the concrete block (concrete beam between hinge regions). BEAM3 is chosen to model the beam element in ANSYS. The BEAM3 element is a uniaxial element with tension, compression, and bending capabilities. The element has three degrees of freedom at each node: translations in the nodal x and y directions and rotation about the nodal z-axis (Figure 3-6). The geometry (width, height, length) and the material parameters (Young's modulus, Poisson's ratio) are used to define this element.

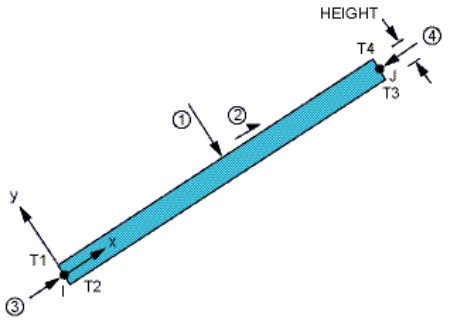

Figure 3-6. BEAM3 element (ANSYS 2005)

3.3.2 Concrete compression and steel tension spring

The concrete compression spring and steel tension spring from the moment couple to model the moment rotation at the end of the beam. The element COMBIN39 (Figure 3-7)

is chosen to model these two springs. The element is defined by two node points and a generalized tension-compression force-deflection curve (Figure 3-7). Each node has three degrees of freedom: translations in the nodal x, y, and z directions. The element also has large displacement capability.

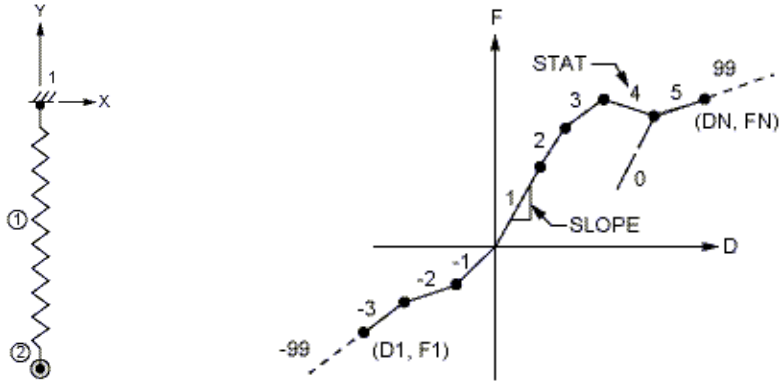

Figure 3-7. COMBIN39 element defined by a tension-compression force-deflection curve (ANSYS 2005)

The properties of the concrete compression and steel tension springs are derived from moment-curvature analysis (Figure 3-8) for the section in the hinge region. The outcome of this analysis is the relation between the concrete compression force Cc, the steel tension force T and the concrete and steel strains. The strain is multiplied by the effective depth of the section (d) to determine the displacements in the spring.

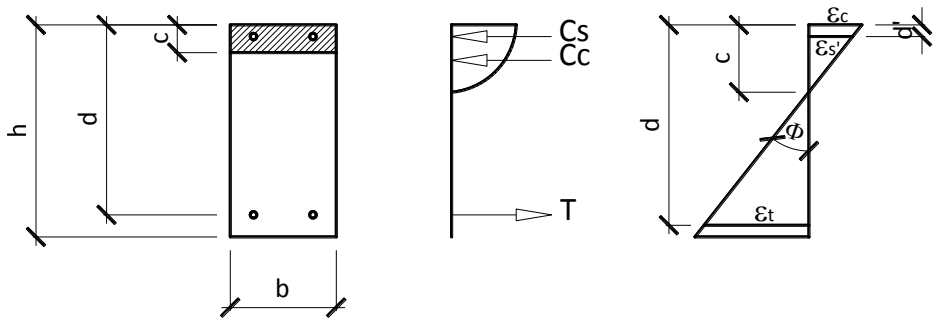

Figure 3-8. Moment-curvature analysis in a concrete section

In Figure 3-8, Cc is compressive force in the concrete which include the compressive force in the compression steel, T is the tension force in the tension steel, ε_c is the compression strain in the concrete, $\varepsilon_{s'}$ is the strain in the compression steel, and ε_t is the strain in the tension steel.

The combination of concrete compression and steel tension spring replicates the moment rotation behavior in the hinge. Figure 3-9 and Figure 3-10 show examples of force-displacement curves results of the concrete compression spring and the steel tension steel for a reinforced concrete beam with continuous reinforcement (Orton 2007).

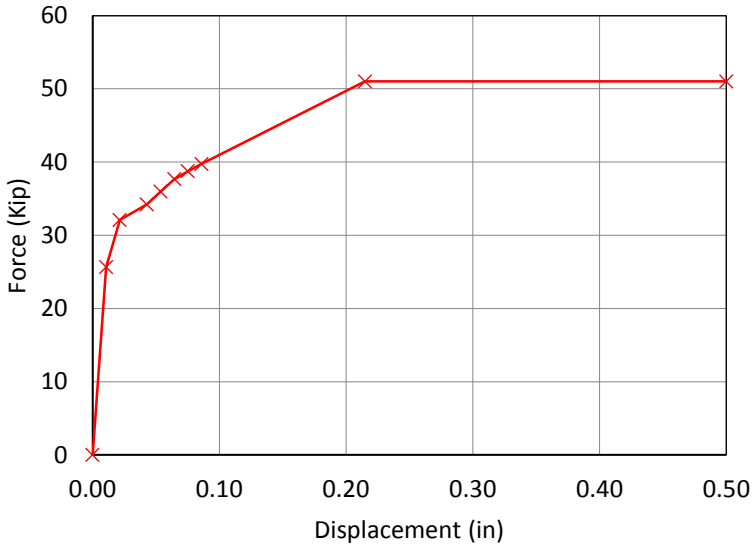

Figure 3-9. Force – displacement curve example of a concrete compression spring for a reinforced concrete beam with continuous reinforcement (Orton 2007).

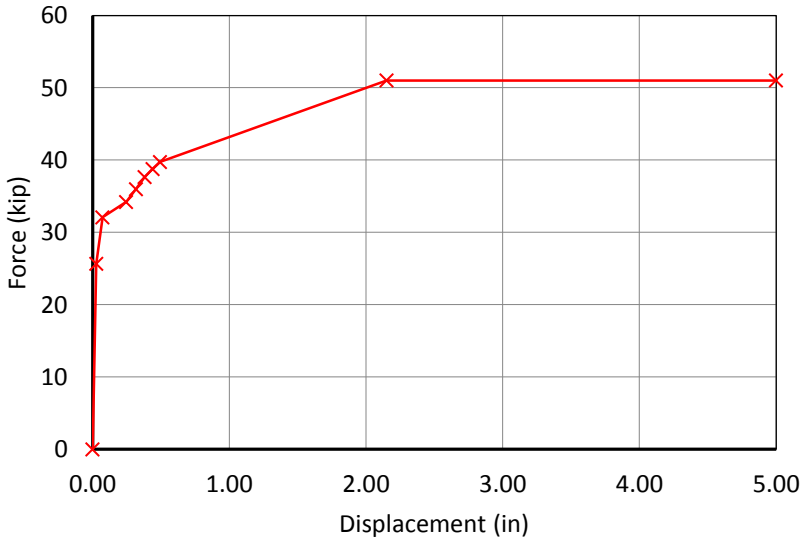

Figure 3-10. Force – displacement curve example of a steel tension spring for a reinforced concrete beam with continuous reinforcement

3.3.3 Axial Extension Spring

One of the key elements of the simplified model is the axial extension spring. It represents the axial extension that occurs within the beam. The axial extension controls the slope of the load deflection response of the beam during catenary action. The same COMBIN39 element as the concrete compression and steel tension spring is used for this element. The following paragraphs explain the steps followed to define the force displacement relationship of the axial extension spring and the method adopted.

First, a comparison is made between the tension properties of the axial extension spring back-calculated from experimental data from Orton's test NM-1 and the tension properties of the same area of steel under uniform axial tension (based on stress strain curve of steel). As can be seen in Figure 3-11 the comparison between the two shows that both indicate the same level of yield of the reinforcement (at about 32 kips of axial tension), however the strain (or displacement) at which the yield occurs is much larger in the experimental test data. The reason for this difference comes from the fact that the stress in the steel under catenary action is not uniform due to effects from the concrete and moments applied to the beam.

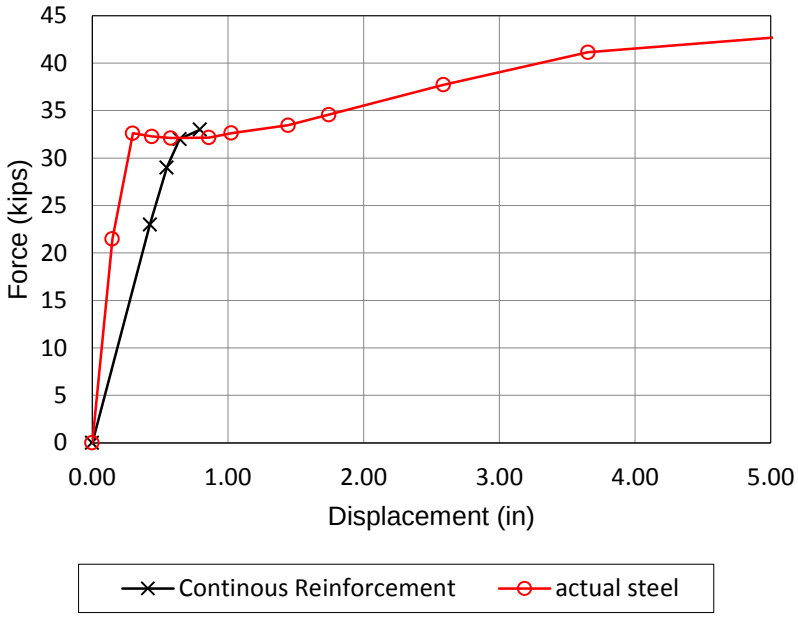

Figure 3-11. Force-displacement curves of the axial extension spring from experimental data from Orton's test NM-1 and a piece of steel under uniform axial tension.

Figure 3-12 shows strain gage readings from Orton's test NM-2 (similar to NM-1). These gages indicate that as the distance from the removed column increases, the axial tension when the gage reaches yield also increases. Or, that not all of the reinforcement reaches yield at the same time, with some gages reaching yield much before the predicted yield capacity of 32 kips. Therefore the yielding (and stress) varies along the length of the beam. This helps explain the difference between the results for the axial extension spring properties from the experimental results and the stress-strain curve of the same area of steel under a uniform axial tension. Therefore, because of the distributed yielding along the length of the beam the initial slope of the force deformation curve is shallower as some sections of steel yield early. Then, as a greater percentage of the steel reaches yield the curve starts to flatten out.

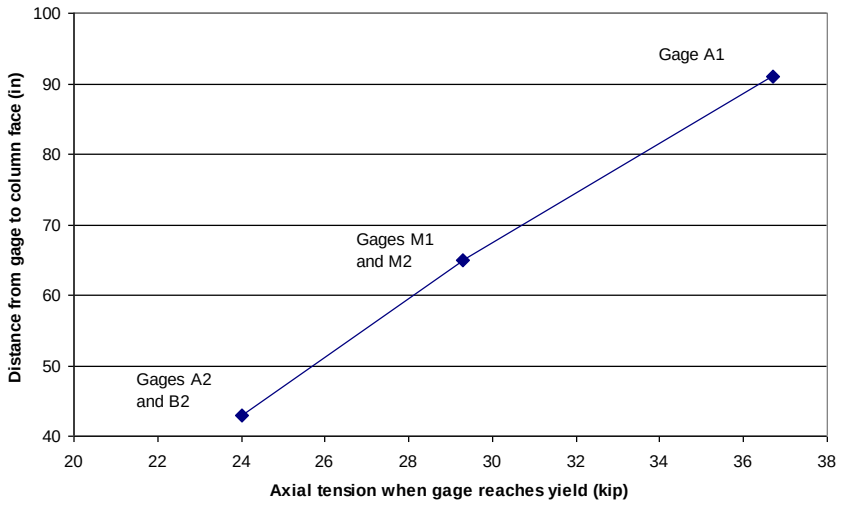

Figure 3-12. Variation of yielding along beam (NM-2), Orton (2007)

In order to find a way to approximate the axial extension behavior of a reinforced concrete beam under catenary action, it was decided to attempt to use modified equations for the stress strain behavior of steel. These equations are the Ramberg-Osgood (1943) equation (Equation 3-1) which approximates the stress strain behavior of steel as a smooth non-linear curve, and the Sargin (1971) equation (Equation 3-2, 3-3 and 3-4) which uses a piece-wise non-linear function to better approximate the yield plateau.

The Ramberg-Osgood equation has the form:

$$\varepsilon_s = \frac{\sigma_s}{E_s} + \frac{\varepsilon_{sp}}{\sigma_{sp}^{n_s}} \sigma_s^{n_s} \tag{3-1}$$

Where E_s is the elastic modulus, ε_{sp} is the strain in the plastic region, σ_{sp} is the stress in the plastic region, and n_s is a parameter that depend on the material considered.

The Sargin equation has the form:

$$f_s = E_s\varepsilon_s \quad \text{for} \quad 0 \le \varepsilon_s \le \varepsilon_y \tag{3-2}$$

$$f_s = f_y \quad \text{for} \quad \varepsilon_s \le \varepsilon_s \le \varepsilon_{sh} \tag{3-3}$$

$$f_s = f_y + E_{sh}(\varepsilon_s - \varepsilon_{sh})\left[1 - \frac{E_{sh}(\varepsilon_s - \varepsilon_{sh})}{4(f_{su} - f_y)}\right] \quad \text{for} \quad \varepsilon_s > \varepsilon_{sh} \tag{3-4}$$

Where f_s and ε_s represent stress and strain in the steel in general, the subscript y refers to yielding, the subscript sh refers to strain hardening, and the subscript su to ultimate or maximum stress.

The equations, with parameters listed in Table 3-1 and Table 3-2, are compared to an experimental test on a piece of steel from the Orton data, Figure 3-13. These equations are able to accurately reproduce the stress-strain behavior of steel.

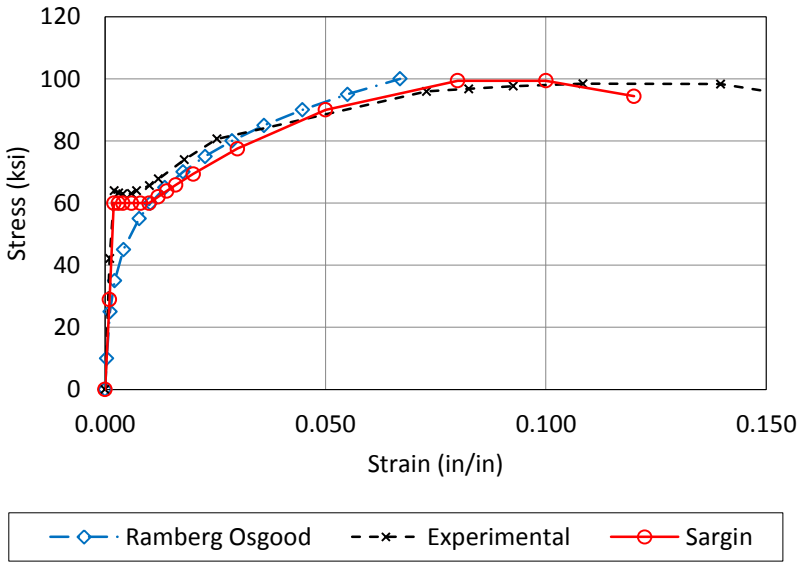

Figure 3-13. Steel stress-strain curves from Orton's data, Ramberg-Osgood and Sargin equation.

Table 3-1 Ramberg-Osgood parameters

ε_{sp} [in/in]	0.01
σ_{sp} [ksi]	63
n_s	4

Table 3-2. Sargin parameters

ε_y [in/in]	0.002
ε_{sh} [in/in]	0.01
E_{sh} [ksi]	1,000
f_y [ksi]	60
f_{su} [ksi]	100
E [ksi]	29,000

The next step is to modify the parameters in the equations in order to replicate the experimental force-deflection behavior of a reinforced concrete beam under catenary action.

For reinforced concrete beam with continuous reinforcement, Figure 3-14 compares the force-displacement curves back calculated from experimental data, and for the modified Ramberg-Osgood and Sargin equations. For reference a curve for the unmodified behavior of a piece of steel is also shown.

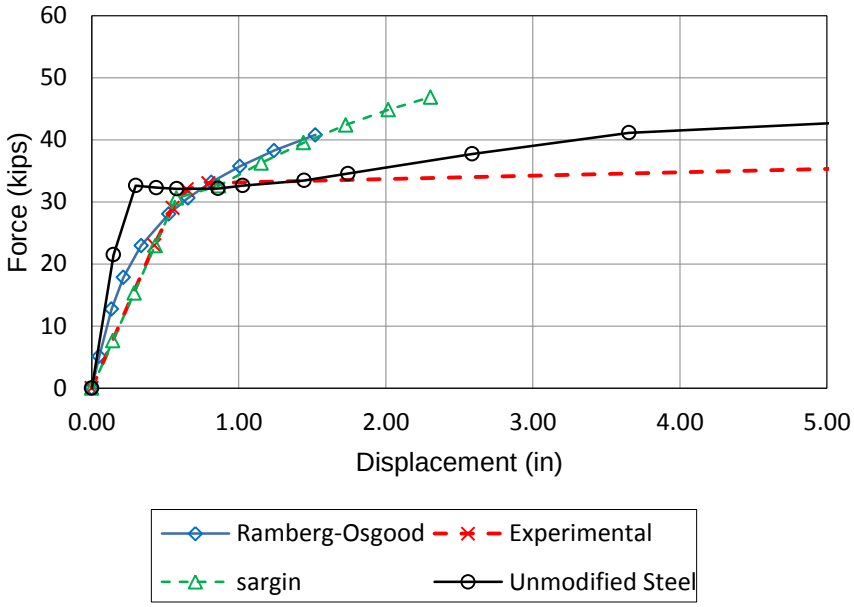

Figure 3-14. Force-displacement curves of model with continuous reinforcement from Orton's experimental data, the modified Ramberg-Osgood and the Sargin equation.

The parameters for the modified Ramberg-Osgood and Sargin equations are summarized in Table 3-3:

Table 3-3. Ramberg-Osgood and Sargin parameters for model with continuous reinforcement

		Unmodified	Modified
Ramberg-Osgood	εsp (in/in)	0.01	0.003
	σsp (ksi)	63	63
	ns	4	4
Sargin	ε_y	0.002	0.005
	ε_{sh}	0.01	0.005
	E_{sh}	1,000	4000
	f_y	60	60
	f_{su}	100	100
	E	29,000	15000

For the Ramberg-Osgood equation the ε_{so} parameter is changed from 0.01 to 0.003 which essentially steepens the initial part of the Ramberg-Osgood curve. This is important because the unmodified Ramberg-Osgood curve does not closely follow the actual stress strain behavior of the steel when it is near the yield plateau. By changing the value of ε_{so} a better approximation is made early in the stress strain curve.

Because the Sargin equation better replicated the early stress strain behavior of steel, more information can be learned by its changed parameters. For the Sargin equation the strain at which yielding begins (ε_y) is adjusted from 0.002 to 0.005 and the strain in the strain hardening region is also adjusted from 0.01 to 0.005. This essentially says that the yielding does not start until later (as was evidenced by the experimental data) and the specimen immediately goes into strain hardening. The elastic Young's modulus E is also changed so that "yielding" occurring at 0.005 will still occur at a stress of 60 ksi. The strain hardening modulus is increased from 1000 ksi to 4000 ksi because of the distribution of stress in the beam. This distribution causes some sections of the steel to be in the elastic region while others are in strain hardening. Therefore, the effective strain hardening modulus is increased.

For reinforced concrete beam with non-continuous reinforcement, Table 3-13 compares the force-displacement curves back calculated from experimental data, and for the modified Ramberg-Osgood and Sargin equations.

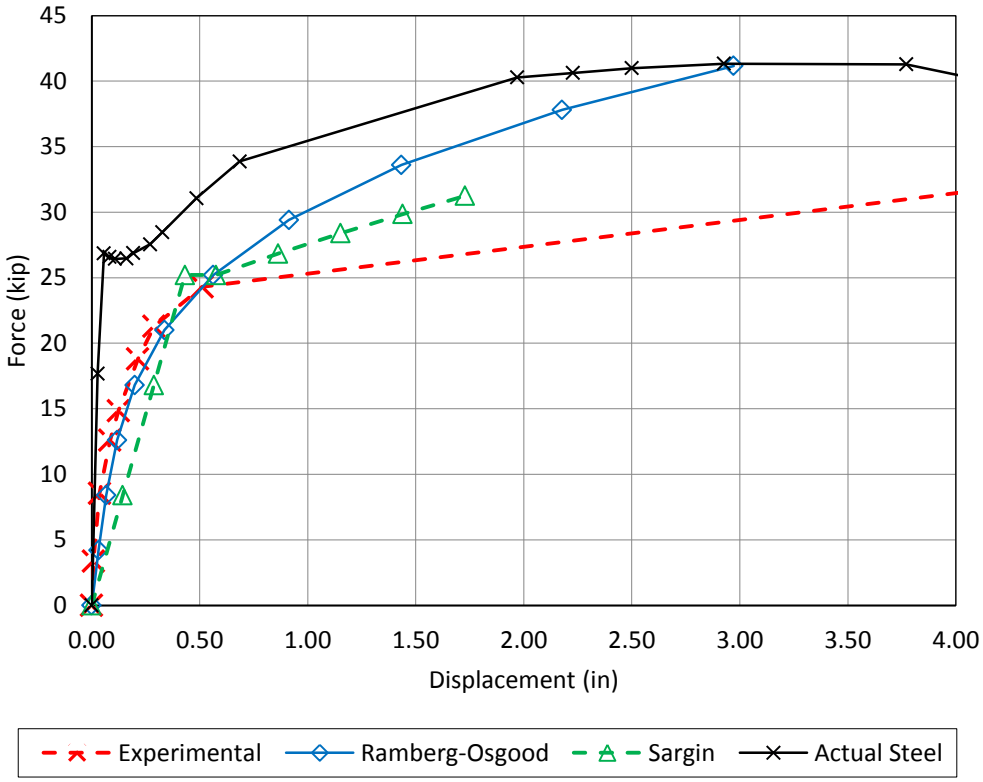

Figure 3-15. Force-displacement curves of model with non-continuous reinforcement from Orton's experimental data, the modified Ramberg-Osgood and the Sargin equation.

The parameters for the modified Ramberg-Osgood and Sargin equations are summarized in Table 3-4:

Table 3-4. Ramberg-Osgood and Sargin parameters for model with non-continuous reinforcement

		Unmodified	Modified
Ramberg-Osgood	εsp (in/in)	0.01	0.005
	σsp (ksi)	63	60
	ns	4	4
Sargin	ε_y	0.002	0.004
	ε_{sh}	0.1	0.004
	E_{sh}	1,000	2,000
	f_y	60	60
	f_{su}	100	100
	E	29,000	20,000

For the Ramberg-Osgood equation the ε_{so} parameter is changed from 0.01 to 0.005 which steepens the initial part of the Ramberg-Osgood curve. This is the same modification that was made for the beam with continuous reinforcement. Therefore, in terms of the Ramberg-Osgood equation, there is no difference in the beam with continuous reinforcement and one without continuous reinforcement.

For the Sargin equation the strain at which yielding begins (ε_y) is adjusted from 0.002 to 0.004 and the strain in the strain hardening region is also adjusted from 0.01 to 0.004. The 0.004 value is a little less than the 0.005 value used for the case with continuous reinforcement. This possibly indicates a more uniform state of stress in the reinforcement or additional deformation due to the transfer of forces from one layer of steel to another. The elastic Young's modulus E is also changed so that "yielding" occurring at 0.004 will still occur at a stress of 60 ksi. The strain hardening modulus is increased from 1000 ksi to 2000 ksi because of the distribution of stress in the beam. Again, because of a more

uniform state of stress in the steel, the Young's modulus does not increase as much as in the beam with continuous reinforcement.

For the compression side of the axial extension spring, the properties of the spring are determined from the properties of concrete. First the compressive stress strain curve for concrete is determined by the commonly used Hognestad (1955) stress strain curve relationship. For the force-displacement curve used in ANSYS, the displacement is calculated by the strain times the length of the beam element. The force is calculated as the stress time the average area of the compressive stress block. Because of limitations in ANSYS, the descending portion of the stress strain curve is not modeled. Therefore, the curve deviates at the highest force, and then continues at a near constant force, Figure 3-16.

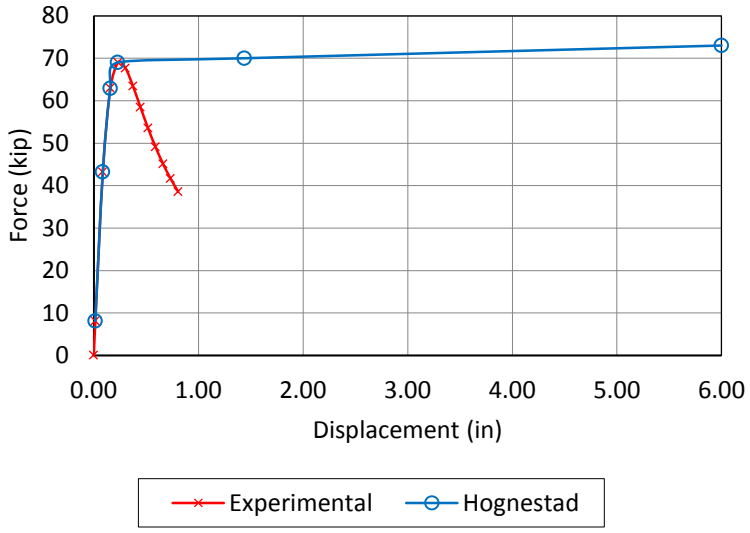

Figure 3-16. Concrete force-displacement curves from experimental data and Hognestad equation

3.3.4 Shear Spring

The shear spring models the shear deformation of concrete in the hinge region. COMBIN39 element is used to represent the shear spring. An equation based on mechanics of materials is used as a basis for developing a constitutive model that enables a user to generate the load-deformation response of the shear spring. The equation is based on the material properties and beam geometry. This equation gives the following relationship between the shear stress τ, shear modulus G and the shear strain γ:

$$\tau = G\gamma \tag{3-5}$$

Where:

$$G = \frac{E}{2(1+\upsilon)} \tag{3-6}$$

$$\gamma = \frac{\delta_s}{L_s} \tag{3-7}$$

L_s - Shear span - hinge length d

δ_s - Shear deformation

The shear stress can be expressed by:

$$\tau = \frac{V}{A} \tag{3-8}$$

Where V is the shear force and A is the cross section area of the concrete beam.

The force-displacement relationship is obtained by combining Equation (3.5) through Equation (3-8). It becomes:

$$V = GA\frac{\delta_s}{L_s} \tag{3-9}$$

Figure 3-17 shows an example of force V versus displacement δ_s curve of a shear spring for a reinforced concrete beam with continuous reinforcement (Orton 2007).

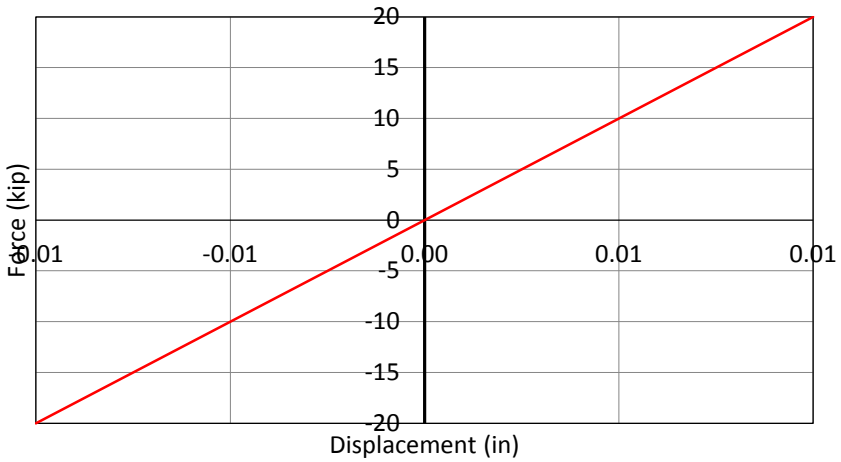

Figure 3-17. Shear spring force-displacement curve for a reinforced concrete beam with continuous reinforcement (Orton 2007).

3.4 Implementation of the simplified models in ANSYS

The finite element analysis commercial code ANSYS is used to implement and simulate the numerical models. Three models, based on Orton (2007), Sasani and Kropelnicki (2007) experimental data, are analyzed, two continuous and one non-continuous reinforcement. The models are analyzed under large deformation transient analysis with ramped loading.

3.4.1 Model with non-continuous reinforcement – Orton beams NR-2 and PM-2

Figure 3-19 and Figure 3-20 show the first model implemented in ANSYS. It is a model with non-continuous reinforcement based on Orton's experimental data NR-2 and PM-2 (2007). The beam element has a 12 in. by 6 in. cross section, and is 96 in. in length. The

reinforcement consisted of #3 (0.11 in2) and #4 (0.2 in2) reinforcing bars with 60 ksi of yield strength.

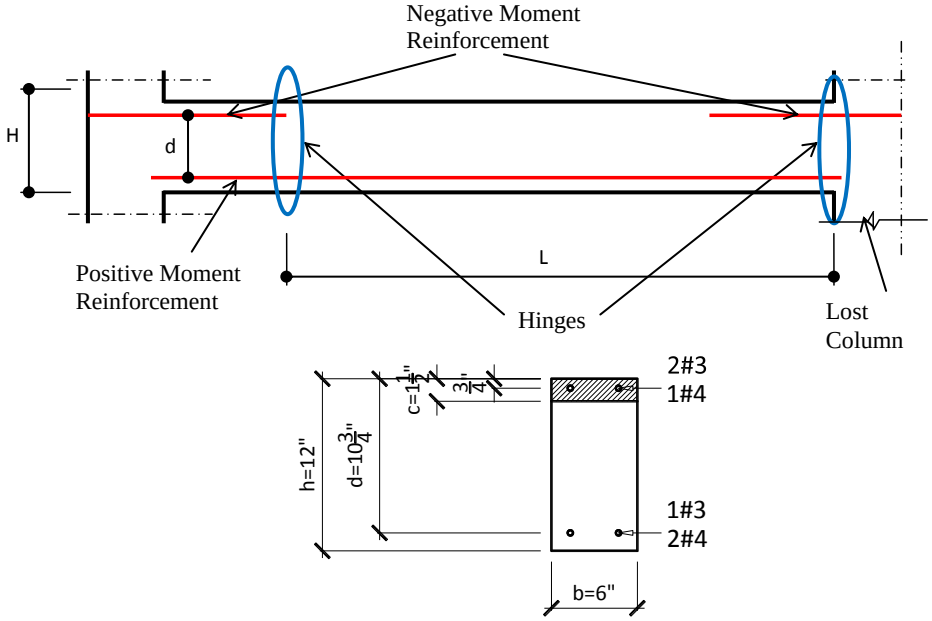

Figure 3-18. Orton beam with non-continuous reinforcement.

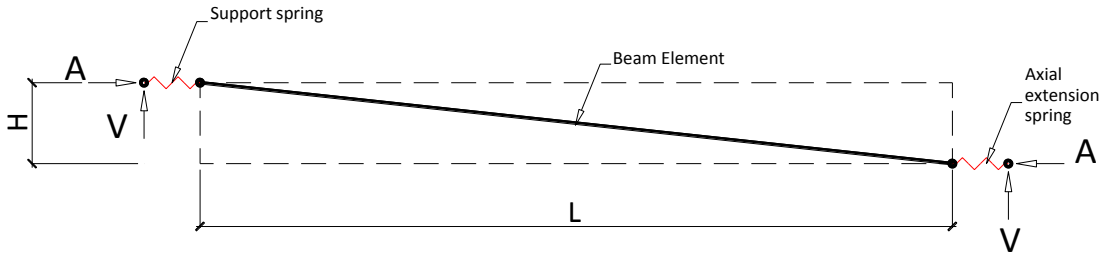

Figure 3-19. Simplified model of the Orton beam with non-continuous reinforcement.

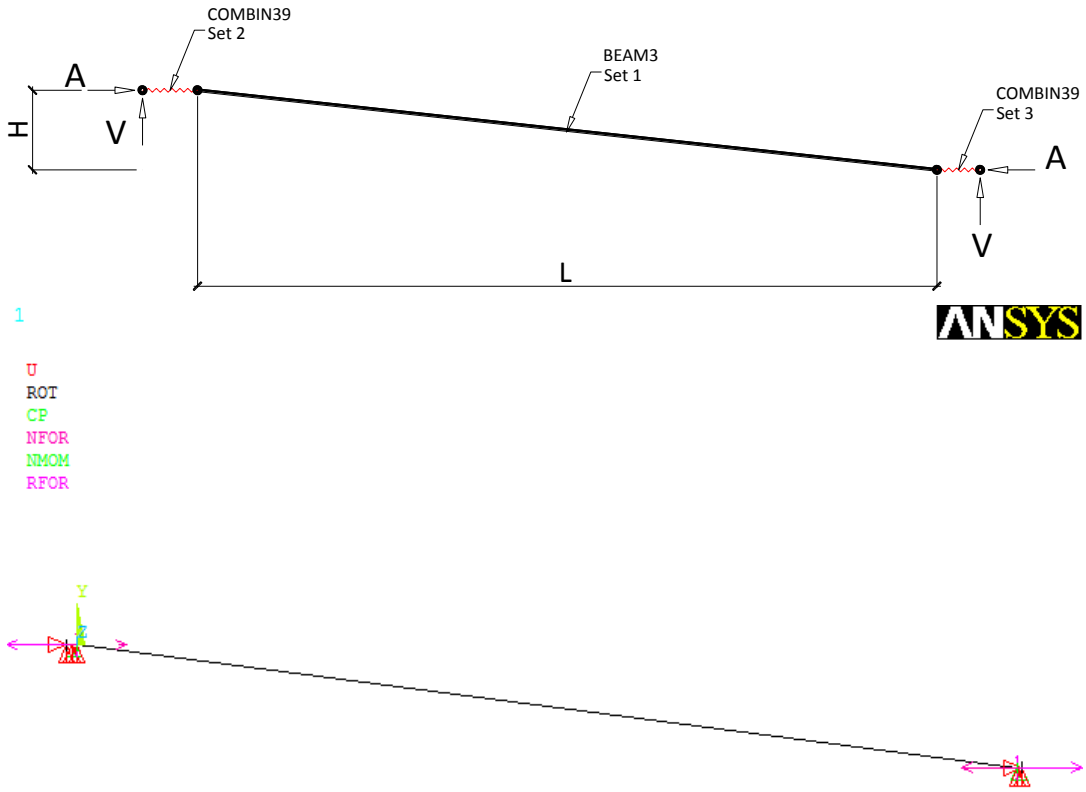

Figure 3-20. Simplified model with non-continuous reinforcement in ANSYS.

The geometry and material properties input for the model are summarized in Table 3-5.

Table 3-5. Geometry and material properties

Geometry			Material		
L	96	in	E	29,000	ksi
h	12	in	At	0.51	in2
b	6	in	As	0.42	in2
d	10.75	in	fy	62	ksi
d'	0.66	in			

The concrete beam (BEAM3 - Set 1) input for the model is summarized in Table 3-6.

Table 3-6. Concrete beam input for Orton beam with non-continuous reinforcement

Cross-sectional area AREA:	72	in2
Area Moment of Inertia IZZ:	864	in4
Total beam height HEIGHT:	10	in

The axial extension spring (Combin39 - Set 2) is calculated based on the information presented in section 3.3.3. The axial extension spring is back calculated from the experimental data, and calculated using the Ramberg-Osgood and Sargin equations for comparisons. The input for the spring data is given in Table 3-7 and a graph of the springs is shown in Figure 3-21.

Table 3-7. Input for axial extension springs for Orton beam with non-continuous reinforcement

	Experimental		Ramberg-Osgood		Sargin	
Material	Displacement	Axial Load	Displacement	Axial Load	Displacement	Axial Load
	in	kip	in	kip	in	kip
Concrete	-6.000	-73.0	-6.000	-73.0	-6.000	-73.0
	-0.191	-67.7	-0.191	-67.7	-0.191	-67.7
	-0.146	-69.0	-0.146	-69.0	-0.146	-69.0
	-0.100	-62.9	-0.100	-62.9	-0.100	-62.9
	-0.055	-43.2	-0.055	-43.2	-0.055	-43.2
	-0.009	-8.1	-0.009	-8.1	-0.009	-8.1
Steel	0.000	0.0	0.000	0.0	0.000	0.0
	0.008	3.4	0.032	4.2	0.144	8.4
	0.036	8.5	0.067	8.4	0.288	16.8
	0.085	12.6	0.118	12.6	0.432	25.2
	0.123	14.8	0.199	16.8	0.576	25.2
	0.213	18.8	0.337	21.0	0.864	26.8
	0.289	21.3	0.563	25.2	1.152	28.4
	0.512	24.3	0.913	29.4	1.440	29.9
	9.150	42.0	1.434	33.6	1.728	31.2
			2.177	37.8	2.016	32.55
			2.972	41.2	2.304	33.768

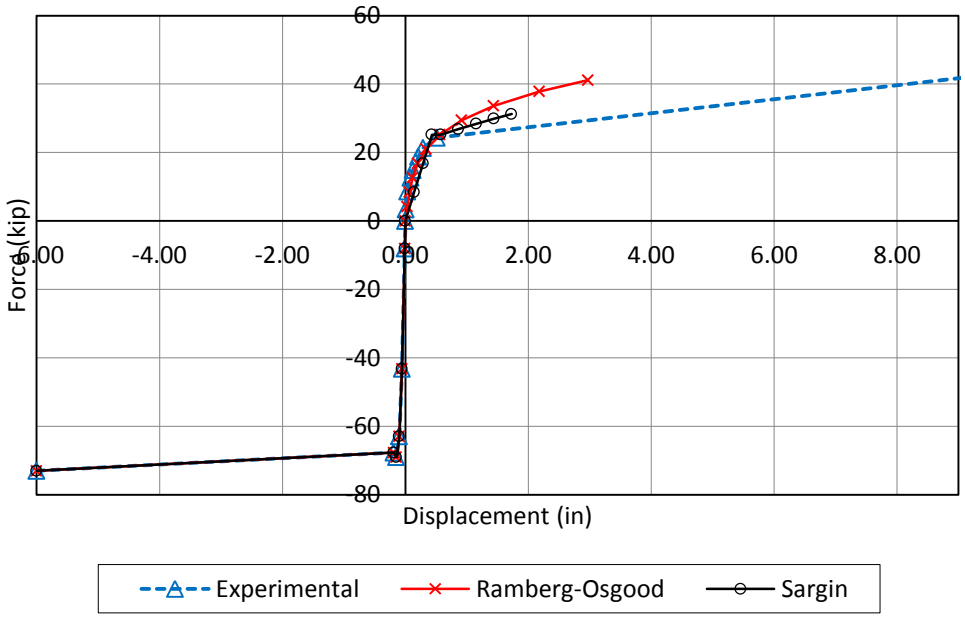

Figure 3-21. Axial extension spring force-displacement curve for Orton beam with non-continuous reinforcement

During testing Orton measured the axial movement at the supports of the beams. A support spring representing this movement is included in the ANSYS model. The support spring (Combin39 - Set 3) input is shown in Table 3-8.

Table 3-8. Support spring input data for Orton tests

Displacement	Force
in	kip
-8	-3
-0.3	-2.5
-0.05	-0.8
0	0
0.4	35

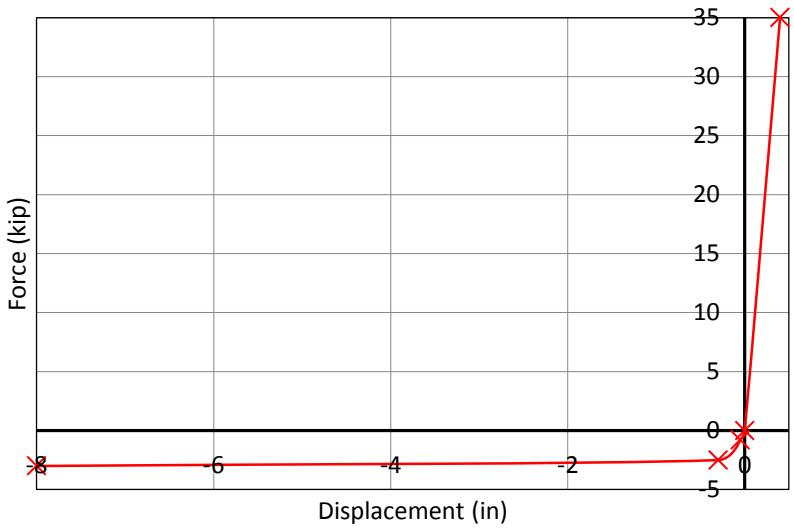

Figure 3-22. Support spring force-displacement curve for Orton beams

3.4.2 Model with continuous reinforcement – Orton beams NM-1 and NM-2

The second model implemented in ANSYS is a model with continuous reinforcement based on Orton's experimental data for tests NM-1 and NM-2 (2007). The beam element has 12 in. by 6 in. cross section, and 144 in. in length. The reinforcement consisted of #3 (0.11 in2) and #4 (0.2 in2) reinforcing bars as shown in Figure 3-23.

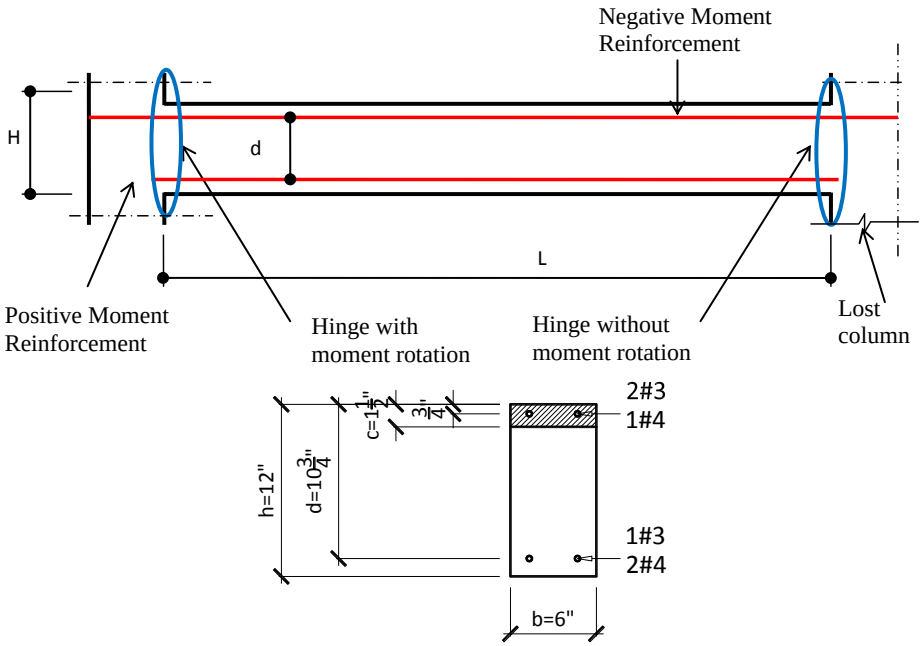

Figure 3-23. Orton beam with continuous reinforcement

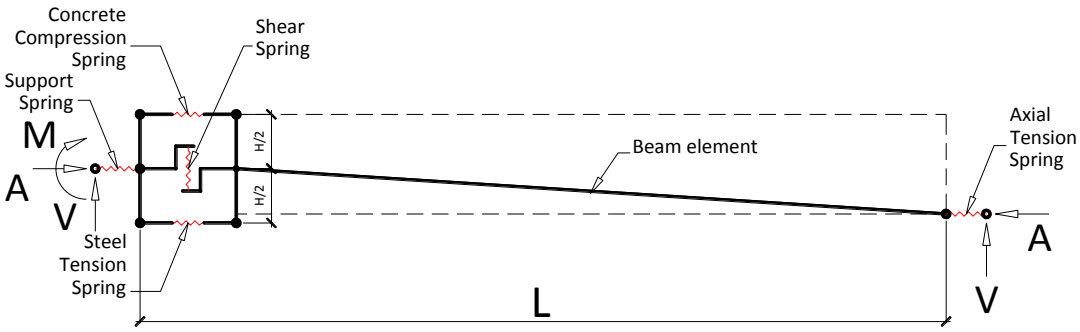

Figure 3-24. Simplified model of the Orton beam with continuous reinforcement.

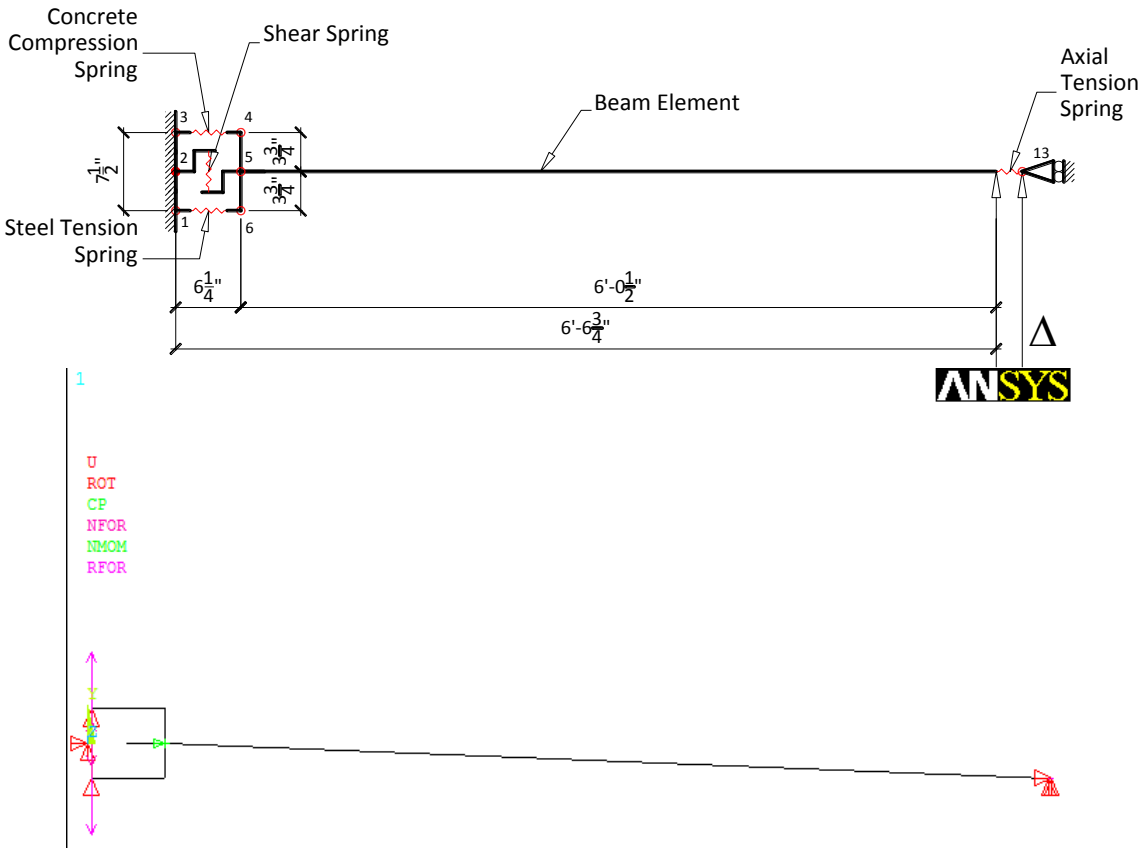

Figure 3-25. Model of the beam with continuous reinforcement in ANSYS

The geometry and material properties input for the model are summarized in Table 3-9 and Table 3-10

Table 3-9. Geometry

L	96	in
h	12	in
b	6	in
d	10.75	in
d'	0.66	in

Table 3-10. Material property

E	29,000	ksi
At	0.51	in2
As	0.42	in2
fy	62	ksi

The concrete beam (BEAM3 - Set 1) input is given in Table 3-11.

Table 3-11. Concrete beam input for Orton beam with continuous reinforcement

Cross-sectional area AREA:	72	in2
Area Moment of Inertia IZZ:	864	in4
Total beam height HEIGHT:	10	in

For beams with continuous reinforcement, moment restraint exists at the section near the support. As presented in section 3.3.2 this moment restraint is represented by a couple of a concrete compression spring and steel tension spring. The concrete compression spring input is summarized in Table 3-12.

Table 3-12. Concrete compression spring input for Orton beam with continuous reinforcement

Displacement in	Force Kip
0.000	0
0.011	26
0.022	32
0.043	34
0.054	36
0.065	38
0.075	39
0.086	40
0.215	51
0.500	51

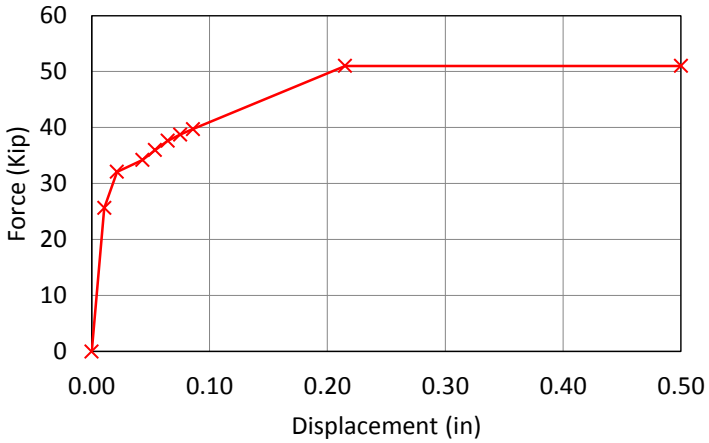

Figure 3-26. Concrete compression spring force-displacement curve for Orton beam with continuous reinforcement

Steel tension spring input is summarized in Table 3-13.

Table 3-13. Input data for steel tension spring for Orton beam with continuous reinforcement

Displacement in	Force kip
0.000	0
0.027	26
0.073	32
0.246	34
0.317	36
0.381	38
0.440	39
0.495	40
2.150	51
5.000	51

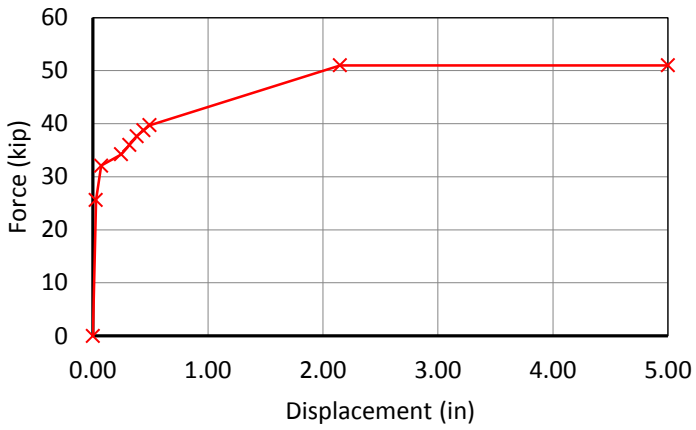

Figure 3-27. Steel tension spring force-displacement curve for Orton beam with continuous reinforcement

The axial extension spring (Combin39 - Set 2) is calculated based on the information presented in section 3.3.3. The axial extension spring is back calculated from the experimental data, and calculated using the Ramberg-Osgood and Sargin equations for comparisons. The input for the spring data is given in Table 3-14 and shown in Figure 3-28.

.

Table 3-14. Input for axial extension spring for Orton beam with continuous reinforcement

	Experimental		Ramberg-Osgood		Sargin	
Material	Displacement	Axial Load	Displacement	Axial Load	Displacement	Axial Load
	in	kip	in	kip	in	kip
Concrete	-6.000	-73.0	-6.000	-73.0	-6.000	-73.0
	-0.191	-67.7	-0.191	-67.7	-0.191	-67.7
	-0.146	-69.0	-0.146	-69.0	-0.146	-69.0
	-0.100	-62.9	-0.100	-62.9	-0.100	-62.9
	-0.055	-43.2	-0.055	-43.2	-0.055	-43.2
	-0.009	-8.1	-0.009	-8.1	-0.009	-8.1
Steel	0.000	0	0.000	0.0	0.000	0.0
	0.425	23	0.050	5.1	0.144	7.7
	0.549	29	0.135	12.8	0.288	15.3
	0.645	32	0.215	17.9	0.432	23.0
	0.795	33	0.336	23.0	0.576	30.6
	10.000	38	0.524	28.1	0.864	32.6
			0.653	30.6	1.152	36.3
			0.812	33.2	1.440	39.5
			1.006	35.7	1.728	42.4
			1.240	38.3	2.016	44.8
			1.521	40.8	2.304	46.9

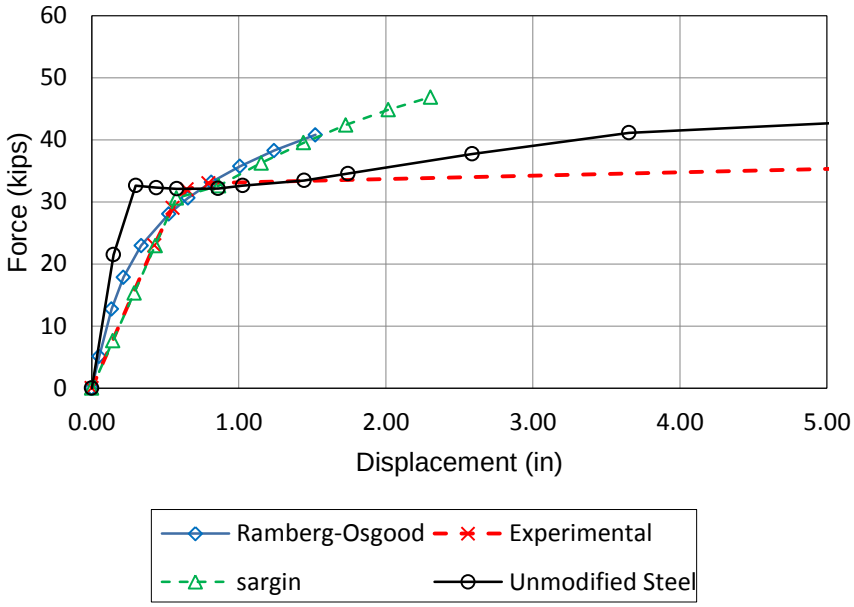

Figure 3-28. Axial extension spring force-displacement curve for Orton beam with continuous reinforcement

The support spring (Combin39 - Set 3) input and shear spring input is the same as for the Orton beam without continuous reinforcement.

3.4.3 Model with continuous reinforcement – Sasani and Kropelnicki (2007)

The third model implemented in ANSYS is a beam element part of an experimental program carried out by Sasani and Kropelnicki (2007). The beam has fixed boundaries and is 13ft 8 1/4 in. long with a cross-section of 12 in. by 20 in. The reinforcement is continuous. The detailing is shown in Figure 3-29. Reinforcement of grade 75 ksi was used along with concrete compressive strength of 6 ksi.

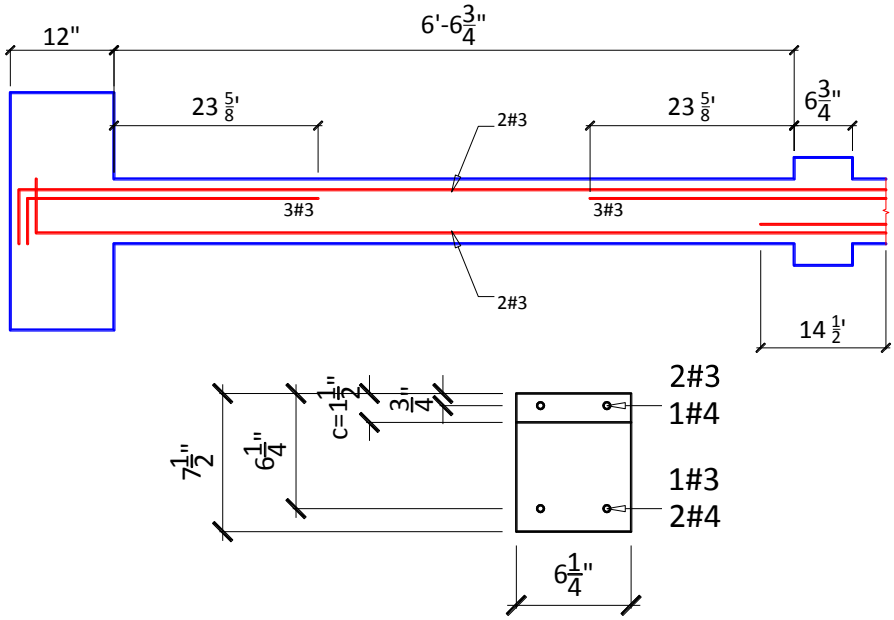

Figure 3-29. Reinforcement detailing of Sasani and Kropelnicki's experimental beam (Sasani and Kropelnicki, 2007).

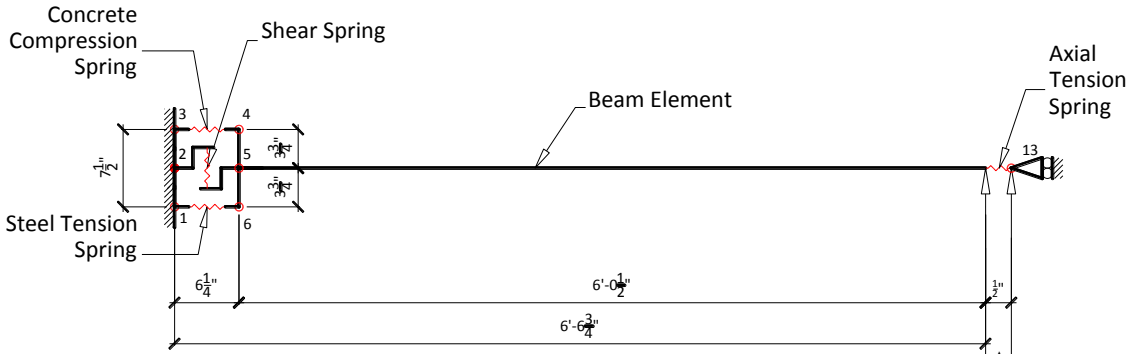

Figure 3-30. Simplified model of Sasani and Kropelnicki's beam.

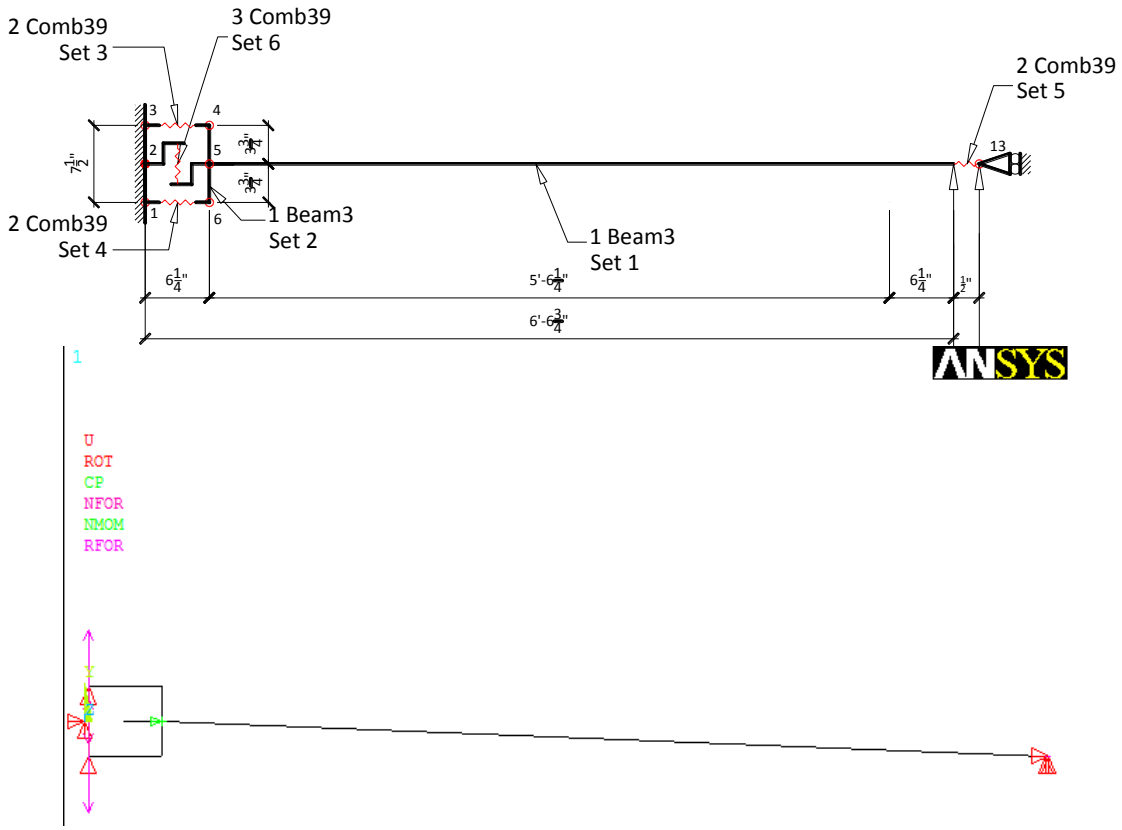

Figure 3-31. Simplified model in ANSYS

The concrete beam (BEAM3 - Set 1) input is summarized in Table 3-15.

Table 3-15. Concrete beam input for Sasani and Kropelnicki beam

Cross-sectional area AREA:	28	in2
Area Moment of Inertia IZZ:	6667	in4
Total beam height HEIGHT:	7.5	in

For beams with continuous reinforcement, moment restraint exists at the section near the support. As presented in section 3.3.2 this moment restraint is represented by a couple of a concrete compression spring and steel tension spring. The concrete compression spring (2 Comb39 - Set 3) input is summarized in Table 3-16.

Table 3-16. Concrete compression spring input for Sasani and Kropelnicki beam

Displacement in	Force Kip
0.000	0
0.007	28
0.013	35
0.026	37
0.033	39
0.040	41
0.046	42
0.053	43
0.132	55
0.500	55

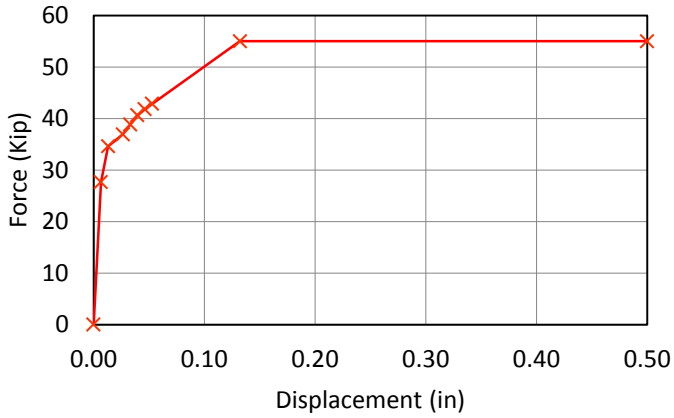

Figure 3-32. Concrete compression spring force-displacement curve - Sasani and Kropelnicki (2007)

The steel tension spring (2 Comb39 - Set 4) input is summarized in Table 3-17.

Table 3-17. Steel tension spring input for Sasani and Kropelnicki beam

Displacement in	Force kip
0.000	0
0.010	28
0.019	35
0.047	37
0.073	39
0.099	41
0.119	42
0.128	43
0.500	55
5.000	55

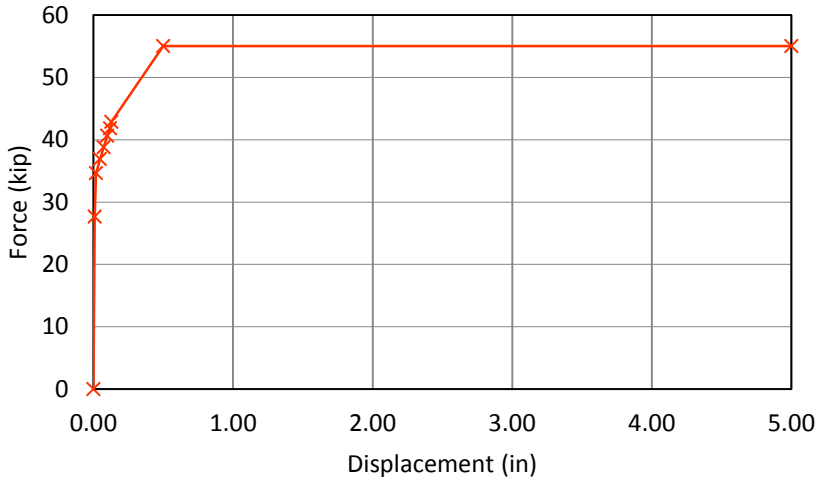

Figure 3-33. Steel tension spring force-displacement curve- Sasani and Kropelnicki (2007)

The axial extension spring (Combin39 - Set 2) is calculated based on the information presented in section 3.3.3. Based on the results of the Orton beam with continuous reinforcement it was decided to use only the Sargin equation for the Sasani and

Kropelnicki beam. The axial extension spring (2 Comb39 - Set 5) input is given in Table 3-18 and shown in Figure 3-34.

Table 3-18. Axial extension spring input for Sasani and Kropelnicki beam

Material	Displacement in	Axial Load kip
Concrete	6	25
	0.151	23.8
	0.115	24.2
	0.079	22.1
	0.043	15.2
	0.007	2.8
Steel	0.000	0.0
	0.072	14.4
	0.144	28.9
	0.216	43.3
	0.288	57.8
	0.432	64.8
	0.576	70.4
	0.720	74.7
	0.864	77.6
	1.008	79.1
	1.152	79.2

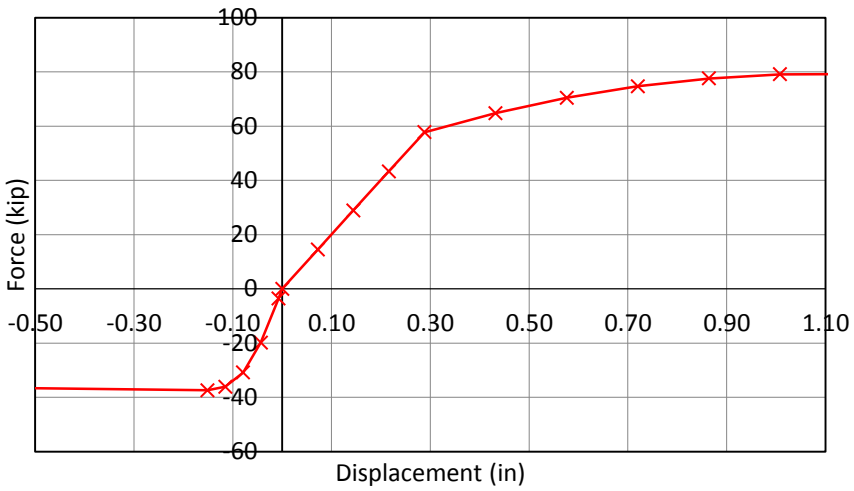

Figure 3-34. Axial extension spring force-displacement curve for Sasani and Kropelnicki beam

The shear spring (3 Combin39 - Set6) input is summarized in Table 3-19.

Table 3-19. Shear spring input for Sasani and Kropelnicki beam

Displacement in	Force kip
-0.01	-20.0
0.0	0.0
0.01	20.0

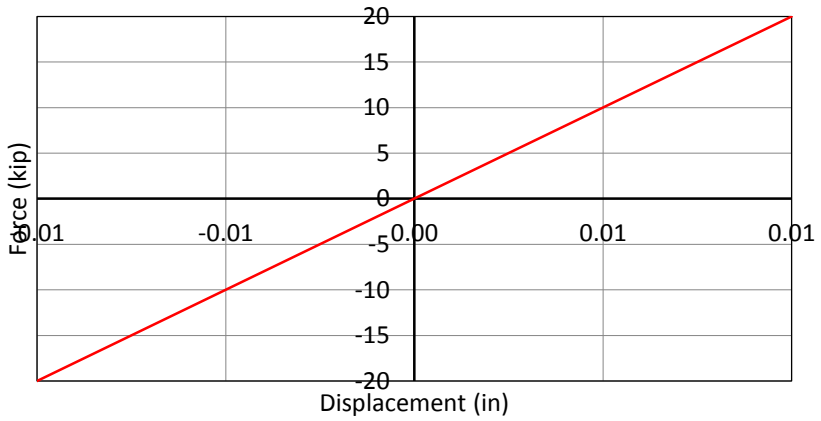

Figure 3-35. Shear spring force-displacement curve for Sasani and Kropelnicki beam

4. COMPARISON OF SIMPLIFIED MODEL RESULTS AND PREVIOUS EXPERIMENTAL TEST RESULTS

The responses from the simplified model are compared and validated using Orton (2007), Sasani and Kropelnicki (2007) experimental data. This chapter compares and discusses the results of the analysis from ANSYS and these experimental data.

4.1 Model with non-continuous reinforcement – Orton beams NR-2 and PM-2

Figure 4-1 and Figure 4-2 shows the results of the model for non-continuous reinforcement defined in ANSYS using the properties presented in section 3.4.1 experimental test data from Orton's tests NR-2 and PM-2.

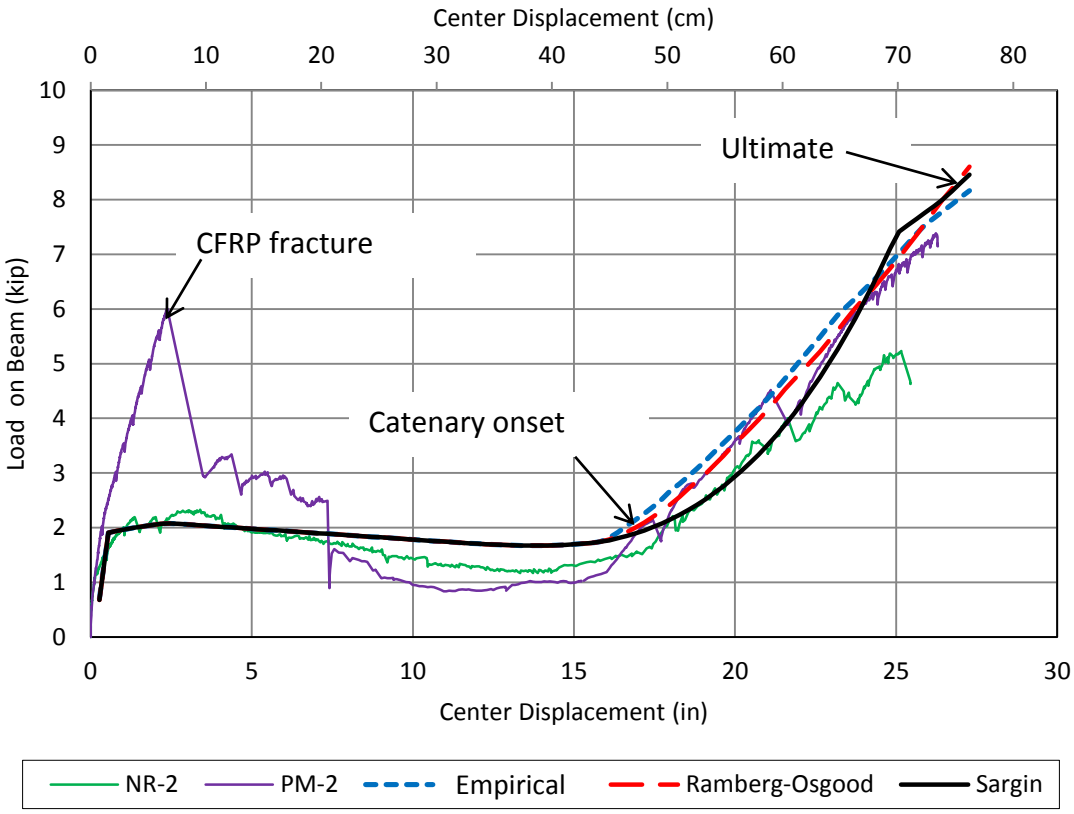

Figure 4-1. Vertical load-central displacement curve of Orton's test and simplified model for non-continuous reinforcement

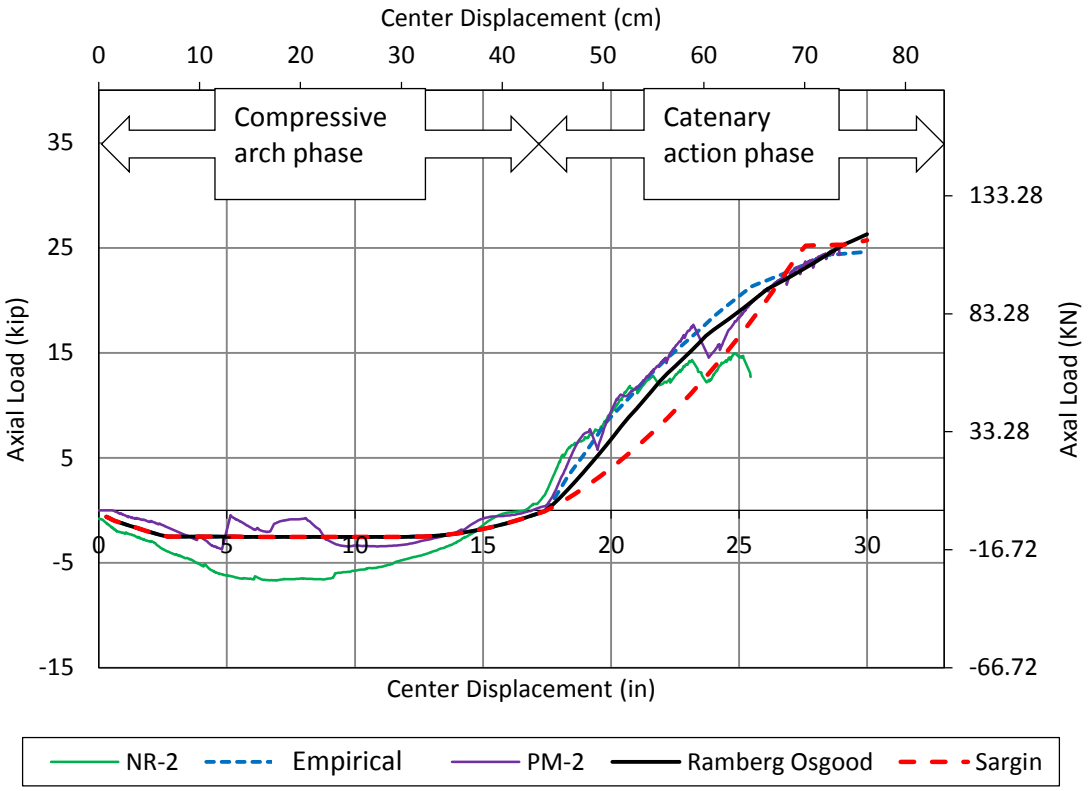

Figure 4-2. Axial load-central displacement curve of Orton's test and simplified model for non-continuous reinforcement

For Orton's specimen PM-2, CFRP was applied to provide continuity of the positive moment reinforcement. During testing this CFRP fractured next to the missing column at 6 kips of load. After the CFRP fracture the specimen behaved like specimen NR-2 which had non-continuous reinforcement. For both NR-2 and PM-2 hinges formed at the sections where the reinforcement terminated (see Figure 3-4). The beam underwent a compressive arch phase until about 16 in. of displacement. Afterwards, the specimen picked up catenary tension until the testing was stopped at about 30 in. of displacement.

The simplified model was able to accurately predict both the vertical and axial loads vs displacement. The spring data back calculated from the experimental data and the modified Ramberg-Osgood equation both produced very accurate results. The Sargin equation is not as accurate, containing a slightly different curvature than the other two curves. This is due to the fact that the initial portion of the axial extension spring data for the Sargin curve is linear whereas the initial portion of the experimental and Ramberg-Osgood curves are curved (see Figure 3-21). This produces some inaccuracy in the test results. It also indicates that although the tension in the beam is at a low level, the axial extension is not linear (as would be expected for steel in its elastic range).

4.2 Model with continuous reinforcement – Orton beams NM-1 and NM-2

Figure 4-3 and Figure 4-4 shows the results of the model for continuous reinforcement defined in ANSYS using the properties presented in Section 3.4.2 and experimental test data from Orton's tests NM-1 and NM-2.

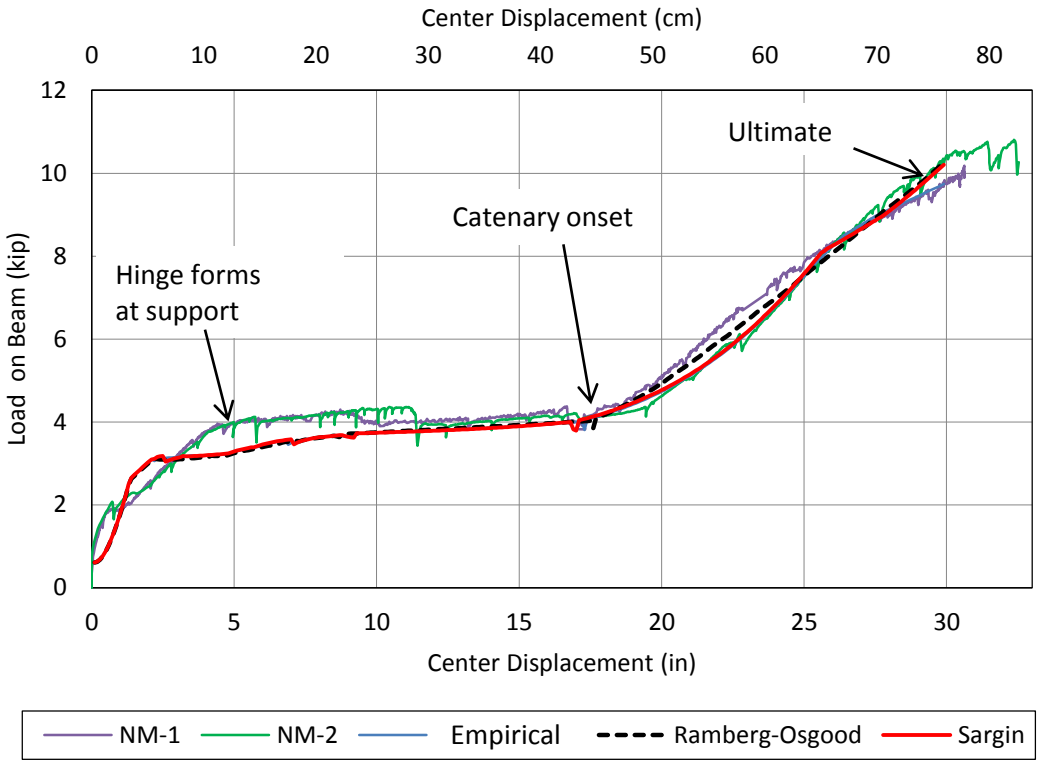

Figure 4-3. Vertical load-central displacement curve of Orton's test and simplified model for continuous reinforcement

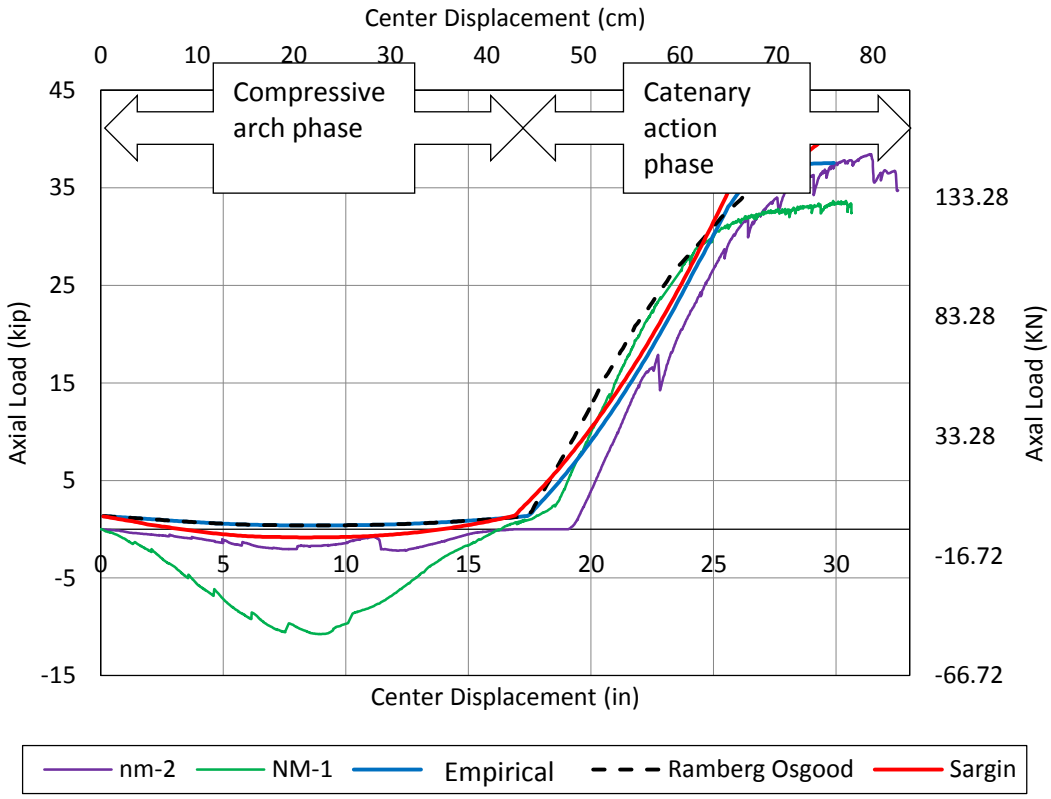

Figure 4-4. Axial load vs central displacement curve of Orton's test and simplified model for continuous reinforcement

From the comparison of the tested data and the simulation results, it is concluded that the simplified model represents well the vertical and axial loads vs displacement. Test results provided shown in Figure 4-3 by Orton (2007) indicate that the hinge at the support reached its maximum moment capacity at a displacement of about 6 in. with 4 kips of vertical load. Then, the catenary tension started at about 17 in of displacement with 4 kip of axial load. The beam reached ultimate at about 30 in of displacement and 10 kip of axial load. In Figure 4-4, the tested beam underwent compressive arch action until a displacement of about 16 in then went to catenary tension up until a vertical displacement

of 30 in and an axial tension of 35 kip before failure. The proposed model represents a close agreement of all these aspect of the beam response. Furthermore, there was little difference in the response of the models for the three different axial spring definitions (experimental, Ramberg-Osgood, and Sargin).

4.3 Model with continuous reinforcement – Sasani and Kropelnicki beam

Figure 4-5 shows the results of the model for continuous reinforcement defined in ANSYS using the properties presented in Section 3.4.3 and experimental test data from Sasani and Kropelnicki (2007).

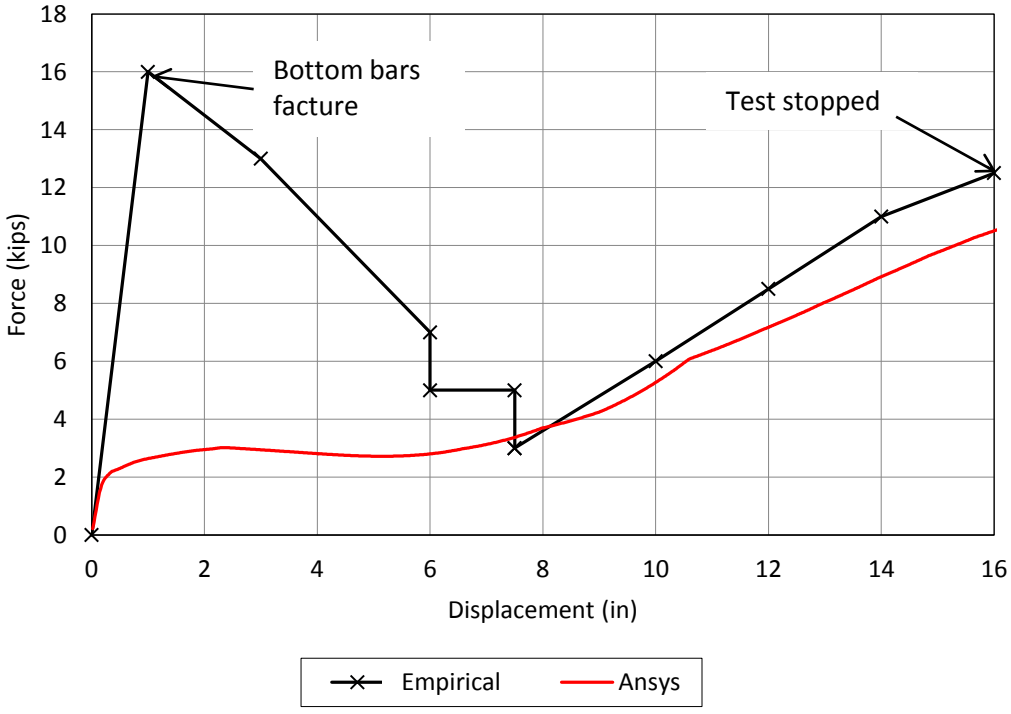

Figure 4-5. Force-displacement curve of Sasani and Kropelnicki's test and simplified model.

During Sasani and Kropelnicki's experiment (Figure 4-5), the two bottom bars fractured at a vertical displacements of about 6.0 in. and 7.5 in. Following the bar fractures, catenary action provided by the top reinforcement results in the increasing resistance of the beam. At a vertical displacement of about 8.5 in the top continuous bars at the center of the beam yielded in tension. The test was stopped at 16 in. of vertical deformation due to geometric constraints.

The simplified model only models the response of the beam after the fracture of the two bottom bars. It represents quite well the catenary phase of the response which is the focus of this research. The model was able to accurately predict the load and displacement at which catenary action begins. Afterward, the slope of the model's curve is shallower than the experimental data. This might be due to the fact that in the experimental test, the reinforcement fractured on only one side of the column resulting in unsymmetrical loading of the beam.

5. CONCLUSIONS

5.1 Conclusion

A simplified model was developed for use in simulating the response of reinforced concrete beams under catenary action. The simplified model was developed based on material properties, geometric constraints, and the reinforcement detailing of the beam. The proposed simplified model included a beam element and a system of springs that represents the load extension behavior and moment rotation behavior of a reinforced concrete beam element. The tensile definition of the axial extension spring was approximated by a steel stress-strain curve modified to account for uneven stress in the steel along the length of the beam. Two types of models were created: to model beams with non-continuous and beams with continuous negative moment reinforcement. The simplified model was analyzed using the commercial finite element analysis code ANSYS. The results of the models are then compared to Orton (2007) and Sasani and Kropelnicki (2007) experimental tests on reinforced concrete beams. It was found that the models predict accurately predict accurately the response of reinforced concrete beams under catenary action.

The conclusions drawn from the results of this research are:

- Simplified models, consisting of a series of spring and beam elements, can be used to accurately predict the catenary action behavior of the beam.

- The choice of model depends on the continuity of the reinforcement. Beams with continuous negative moment reinforcement require a model that replicates the moment rotation response at the support. Beams with non-continuous reinforcement have no moment resistance at either end of the beam element.
- The axial extension of the beam can be represented by a modified stress-strain curve for steel. The modification adjusts for the non-uniform distribution of stress along the reinforcement in the beam. For beams with continuous steel, the modification effectively delays the onset of yielding in the steel and eliminates the yield plateau. For beams with non-continuous steel, the modification is similar, but the effective yielding occurs at a lower value of strain.

5.2 Future Research

Future research still needs to be conducted on:

- The simplified models developed in this research needs to be expanded to a complete reinforced concrete frame to evaluate the possible resistance to disproportionate collapse.
- The simplified models need to be compared to more experimental tests on reinforced concrete beams under catenary action. This will further validate the models, or suggest possible improvements.
- A parametric study needs to be conducted using the simplified models to evaluate the effects of beam geometry, span, and reinforcement details on the catenary response of the beam.

- The simplified models needs to be implemented in programs other than ANSYS (such as SAP) to allow design engineers easier access to the model.
- The simplified model needs to be used to develop design equations for possible use in codes or guidelines.

REFERENCES

Crawford, J.E., (2002). "Retrofit Measures to Mitigate Progressive Collapse," NIST/NIBS Multihazard Mitigation Council National Workshop on Prevention of Progressive Collapse, Chicago,IL, July.

Hognestad, E.; Hanson, N. W.; and McHenry, Douglas, "Concrete Stress Distribution in Ultimate Strength Design," *ACI Journal*, Proceedings V. 52, No.4, Dec. 1955, pp. 455-479.

Izzuddin, B.A., Elghazouli, A.Y. (2004). "Failure of Lightly Reinforced Concrete Members under Fire. I: Analytical Modeling*," Journal of Structural Engineering*, 130(1), pp. 3-17.

Khandelwal, K. and El-Tawil, S. (2006) "Role of Catenary Action during Progressive Collapse of Steel MRF Buildings", St. Louis, MO, United States; 2006. p.35.

Mlakar, P.F., Dusenberry, D.O., Harris, J.R., Haynes G.A., Phan, L.T., and Sozen, M.A.,(2003). "The Pentagon Building Performance Report," *American Society of Civil Engineers*, Reston Virginia.

Nair, R.S. (2004). "Progressive Collapse Basics," <http://www.aisc.org/Content /ContentGroups/Documents/ePubs_Conference_Proceedings/Progressive Collapse Basics.pdf> (Feb. 2, 2006).

Pearson, C. and Delatte, N. (2005) M.ASCE2 "Ronan Point Apartment Tower Collapse and its Effect on Building Codes"*Journal of Performance of Constructed Facilities*,Vol. 19, No. 2, May 1, 2005. ©ASCE, ISSN 0887-3828/2005/2-172–17

Regan, P.E. (1975). "Catenary Action in Damaged Concrete Structures."Industrialization in Concrete Building Construction ACI SP-48, pp191-225.

Sarah Orton (2007) "Development of a CFRP System to Provide Continuity in Existing Reinforced Concrete Buildings Vulnerable to Progressive Collapse" Dissertation, 163-197.

Sargin, M., "Stress-Strain Relationship for concrete and the Analysis of Structural Concrete Sections,". Study No. 4, Solid Mechanics Division, University of Waterloo, Waterloo, Ontario, Canada, 1971, 167 pp.

Sasani, M., Kropelnicki, J. (2007) "Progressive Collapse Anslysis of an RC Structure", The structural Design of Tall and Special Buildings (in press), Wiley Interscience.

Sasani, M. and Sagiroglu, S. (2007) "Progressive Collapse Resistance of Hotel San Diego" *Journal of Structural Engineering*, 134 (4), March 2008, pp. 478-488.

Sucuoglu, H., Citipitioglu, E. Altin, S., (1994), "Resistance Mechanisms in RC Builiding Frames Subjected to Column Failure" *Journal of Structural Engineering*, 120 (3), March 1994, pp. 765-782.

Wang Y.C and Yin, Y.Z (2003) "Analysis of catenary action in steel beams using a simplified hand calculation method, Part 1: Theory and validation for uniform temperature distribution" *J. Constr. Steel Res.*, 61, 183-211.

Yi, W.J., He, Q.F., Xiao, Y. and Kunnath, S.K. (2008) "Experimental Study on Progressive Collapse-Resistant Behavior of Reinforced Concrete Frame Structures" *ACI Structural Journal*, V.105, No. 4, July-August 2008, pp. 433-439.

Wilford, J. C., and Yu, C.W. (1973) "Catenary Action in Damaged Structures" Proceedings of the Department of Environment and CIRIA, Seminar on the Stability of Precast Concrete Structures, London, U.K.e